Book Section:

Torvela, TM orcid.org/0000-0003-1539-8755 (2017) How (not) to recognize a mid-crustal channel from outcrop patterns. In: Law, RD, Thigpen, JR, Merschat, AJ and Stowell, HH, (eds.) Linkages and Feedbacks in Orogenic Systems. The Geological Society of America Memoirs, 213 (213). Geographical Society of America , pp. 129-148. ISBN 9780813782133

https://doi.org/10.1130/MEM213

How (not) to recognize a mid-crustal channel from outcrop patterns

Taija Torvela
University of Leeds, School of Earth and Environment, LS2 9JT, Leeds, UK
t.m.torvela@leeds.ac.uk

ABSTRACT

Mid-crustal channel flow has been hypothesised to be responsible both for the Greater and Lesser Himalayan Sequences (the Miocene Himalayan channel theory), and for the present east- and northward movement and extension of the Tibetan upper crust (the Tibetan middle crustal channel flow theory). As processes within the crust cannot be directly observed, various studies have attempted to validate mid-crustal channel flow by using indirect approaches, including outcrop patterns and other field data from Himalayas, Tibet, and exposed older orogenic roots. The results have been highly debated because arguments can be made that the internal structure of a channel and, therefore, the outcrop patterns of a palaeo-mid-crustal channel are not unique. This paper investigates what types of structural patterns may be produced within a mid-crustal channel, and discusses why they can be difficult, if not impossible, to distinguish from outcrop patterns produced by other mechanisms. A new example from the exposed middle crust of southern Finland is also discussed in this context. While outcrop structural patterns must indeed agree with other potential results that may infer a mid-crustal channel, the inverse is not necessarily true: one cannot infer a mid-crustal channel based on outcrop patterns alone, due to the non-unique nature of the patterns.

INTRODUCTION

The middle crust of the Himalayan-Tibetan system has received increasing attention since the emergence of the mid-crustal channel flow theory which postulates that the partially molten middle orogenic crust is weak enough to "flow" along a differential pressure gradient toward the minimum pressure. Lithospheric-scale mid-crustal flow or channel flow is, in the sense proposed by e.g. Bird, (1991), Clark & Royden (2000), Beaumont et al. (2001), Grujic et al., (1996, 2006), Godin et al., (2006), essentially a mixture of Couette and Poiseuille flows of partially molten material within a sub-horizontal, laterally extensive, lithospheric-scale, mid- to lower lithospheric channel (Fig. 1; Grujic et al., 2002). Channel flow has been hypothesised to be responsible for the deformation and the formation of the inverted metamorphic sequence along the Greater Himalayan Sequence GHS and the Lesser Himalayan Sequence LHS (the Miocene Himalayan extrusion channel theory; Grujic et al., 2002; Searle et al., 2006; see also e.g. Coscombe and Hand, 2000; Dasgupta et al., 2004; Anczkiewicz et al., 2014; Mottram et al., 2014 for descriptions of GHS and LHS). Channel flow has also been suggested to cause the present east- and northward movement and extension of the Tibetan upper crust (the Tibetan middle crustal channel flow theory; e.g. Royden et al., 1997 and 2008; Clark and Royden, 2000). Although melts are known to weaken the rock (e.g. Rosenberg and Handy, 2005), and the middle crust is very likely to play a key role in orogenic processes such as spreading and collapse (e.g. England and Houseman, 1989; Vanderhaeghe and Teyssier, 2001a), relatively little is known of the bulk behaviour of the middle crust: how much melts and other fluids there are, how are they distributed and transported, and, most importantly, how the presence and distribution of melts and other fluids affect the bulk rheology of the middle crust at the scale of the proposed channel flow. As the properties of and processes within the orogenic middle crust cannot be directly observed, various studies have attempted to validate mid-crustal channel flow by using indirect approaches, such as numerical modelling (e.g. Royden et al., 1997; Clark and Royden, 2000; Jamieson et al., 2004 and 2006; Culshaw et al., 2009), outcrop structural patterns and other field data of deformation and metamorphic history from Himalayas, Tibet, and exposed older orogenic roots (e.g. Vanderhaeghe and Teyssier, 2001b; Grujic et al., 2002; Williams and Jiang, 2005; Hatcher and Merschat, 2006; Cagnard et al., 2006; Langille et al., 2010; Searle, 2013), analogue modelling (e.g. Harris et al., 2012), and/or geophysical studies (e.g. Unsworth et al., 2005; Bai et al., 2010; Bao et al., 2015). The results have been highly debated and many authors have examined other evidence and alternative/additional ways of explaining mid-crustal deformation and behaviour, the presence of the GHS, or the movements of the Tibetan upper crust (e.g. Whitney et al., 2004; Leloup et al., 2010; Long and McQuarrie, 2010; Chardon et al., 2011; Wang et al., 2011; Gao et al., 2013).

This paper examines what an exposed palaeochannel, formed by the hypothetical channel flow, might look like at outcrop, and discusses how outcrop patterns from exposed orogenic roots have been used as evidence to validate the mid-crustal channel flow theory, along with the problems with such an approach. The key questions this paper asks are: 1) what outcrop/structural patterns could be expected to result from Couette and/or Poiseuille type channel flow; and 2) are the expected patterns unique to palaeo-mid-crustal channel flow, or can the patterns be equally well or more plausibly explained by other models? The paper does not aim at being an exhaustive review of the theory of channel flow, or of all the processes, scales, and areas that can and have been studied to infer mid-crustal flow: after a brief summary of the necessary properties of mid-crust to induce channel flow, I will discuss examples of potential outcrop patterns that mid-crustal channel flow might produce, based on published field studies and a 3D numerical model of flow in viscous fluid. I will then continue with a brief overview of alternative mechanisms to produce similar outcrop patterns to those presented above. I will also present some new field results from southern Finland in this context. The paper finishes with a discussion on the relationships between the various suggested processes related to the spreading, extension, and/or escape of the middle and lower orogenic crust in general.

MID-CRUSTAL CHANNEL FLOW – PHYSICAL AND GEOMETRIC CHARACTERISTICS

In this chapter, key geophysical and modelling studies inferring partially molten mid-crust on one hand, and the rheological properties of the middle crust on the other hand, are briefly summarized in order to set the background. Similarly, some evidence used to infer potential mid-crustal flow in the Himalayas and Tibet are described, although an exhaustive review is outside a scope of this paper.

For a review of the channel flow theory the reader is referred to e.g. Godin et al. (2006) and Grujic (2006). In short, the channel flow theory suggests that a weak, viscous layer forms in the middle crust of a hot collisional orogen, as a result of heating of and partial melting within the middle/lower crust that is suggested to drastically reduce the rheological strength of this part of the crust (e.g. Beaumont et al., 2004). According to the theory, the pressure gradient resulting from the gravitational potent energy created by lithospheric thickening during the orogenesis, and possibly being enhanced by removal of material through e.g. erosion, causes large-scale lateral displacement or flow in this weak layer (Fig. 1). This flow has been envisaged to be responsible for various phenomena observed in orogens; perhaps most importantly, the Himalayan frontal high-grade metamorphic zone (envisaged to have originally formed in a mid-crustal channel and subsequently exhumed and extruded along the Himalayan front during the Miocene; e.g. Grujic et al., 2002 and 2006); and orogen-parallel spreading and collapse, such as the present north and eastward movement and extension of the Tibetan upper crust and the associated formation of N-S oriented rifts and the North Himalayan gneiss domes, i.e. metamorphic core complexes (both suggested to be at least partially caused by lateral crustal-scale flow within a weak middle crustal layer; e.g. Bird, 1991; Nelson et al., 1996; Clark and Royden, 2000; Beaumont et al., 2004; Zhang et al., 2004; Vanderhaeghe, 2009). In other words, this paper refers to “mid-crustal channel flow” as a pressure gradient –driven, crustal-scale lateral transport of viscous material by Couette-Poiseuille type flow (the contribution of each type varying in time and space), within a laterally extensive layer or channel between two rheologically stronger crustal layers that are moving ("shearing") in opposite directions (Fig. 1; see e.g. Godin et al. 2006 for a more detailed discussion about terminology). This type of flow is, therefore, fundamentally different from other types of middle crustal deformation that are sometimes referred to as “flow”, such as doming, subhorizontal shearing, or (lateral) constrictional deformation: channel flow requires crustal-scale lateral transfer of material along the channel, i.e. necessitates a sufficiently low viscosity that is maintained at the tempo-spatial scale of a mid-crustal channel, in addition to appropriate channel thickness, pressure gradient, and relative velocity between the bounding crustal layers.

This paper considers the internal structure of a mid-crustal channel, but the first-order , diagnostic "boundary conditions" should be mentioned in this context (see Godin et al. (2006) and Jones et al., (2006) for a more detailed summary). These first-order, mostly field-based characteristics include a pair of broadly coeval “roof and floor” shear zones with opposing senses of shear; higher metamorphic grades, reaching anatectic PT conditions, toward the centre of the channel; upper crustal structures cannot be traced through the channel; and pervasive deformation/shearing throughout the channel with early ductile fabrics at the top overprinted by increasingly brittle structures. However, as noted by Jones et al. (2006), these geometric features are characteristic for extrusion of a crustal block(s) in general and are not unique to channel flow, and they may result from other (tectonic) driving mechanisms some of which may be fairly local in nature and unrelated to the formation of a mid-crustal channel at depth. In other words, extrusion may operate independently and the observed geometries may, therefore, be unrelated to channel flow at depth.

In addition to the above patterns, various more ambiguous features have been suggested for the identification of palaeo-mid-crustal channel. For example, although the entire channel is by necessity pervasively deformed/sheared, the strain distribution is likely to vary due to heterogeneous distribution of strain (depending on the scale of observation) and possibly various deformation phases, resulting in discrete deformation planes (shear zones) distributed throughout the channel or even just close to the channel margins (e.g. Grujic et al., 2002; Beaumont et al., 2004). The vorticity and the strain type of the flow is predicted to be complex but, overall, the vorticity is likely to decrease toward the centre of the channel; while the strain type may be either simple shear or general shear, the overall simple shear component is likely to increase toward the channel margins whilst the centre of the channel deforms mainly by pure shear (e.g. Grasemann et al., 1999; Grujic, 2006; Larson and Godin, 2009). An active channel is predicted to be 10-20 km thick in the Tibetan-Himalayan system, although, more generally speaking, narrower channels are possible with an appropriate combination of the key parameters of viscosity, pressure gradient, and bounding layer velocities (e.g. Grujic et al., 1996 and 2006; Clark and Royden, 2000; Beaumont et al., 2004).

Properties of the (Himalayan-Tibetan) middle crust

Typical modern geothermal gradients of c. 20-30°C/km cannot generate large-scale partial melting in a stable, undeforming continental crust of an average thickness of about 35 km (e.g. Petford et al., 2000). Multiple studies show that tectonic perturbation of geotherms and radioactive heat production is needed to induce partial melting, such as happens within orogens (e.g. Thompson and Connolly, 1995; Jamieson et al., 1998). In addition, melting generally requires presence of water (extracted from prograde dehydration reactions) to facilitate melting, producing at most 25% granitic melt from mica-rich pelitic protoliths in the presence of free water (e.g. Thompson and Connolly, 1995). Extensive field evidence from exposed, migmatitic orogenic roots around the world attest that it is probably not unusual for large volumes of partial melts to form in the middle crust of large orogens.

Many geophysical studies from Tibet suggest that significant quantities of melts and/or other fluids are currently present within the mid-crustal zone, below c. 15-20 km depth, although how much actual melts (vs. other fluids) there are remains an open question. A non-exhaustive list of examples is presented here. Francheteau et al. (1984) conducted heat flow measurements in southern Tibet, and interpret the measured high heat flows to indicate recent emplacement of plutonic bodies at depths of maximum 25 km. Makovsky and Klemperer (1999) use three-component wide-angle seismic data from the INDEPTH project to investigate the strengths of P-to-S converted reflections from aligned reflectors at c. 15 km depth in southern Tibet. They conclude that a solid-fluid interface is present at this depth, likely formed by either granitic magma or brine. Kind et al. (1996) examine data from INDEPTH-II passive source experiment and conclude that a mid-crustal low-velocity zone, interpreted as a partially molten layer, is revealed in southern Tibet by inversion of receiver functions, Rayleigh-wave phase velocities, and modelling of the radial component of teleseismic P-waveforms; however, such layer is not observed farther south beneath the Tethyan Himalaya. Nelson et al. (1996) also discuss the INDEPTH-II results to infer that a mid-crustal layer of partial melt exists at least in southern Tibet, but that the thickness and the lateral extent of the layer is unknown; the top of the layer at c. 15-20 km depth is probably complex and transitional, and likely coincides regionally with the wet granite solidus, consistent with the elevated heat flow in southern Tibet. They further suggest that the partial melt layer acts as a decoupling layer and accommodated formation of the south Tibetan core complexes by “lateral mid-crustal flow” (however, not defining what “flow” means in this context), and that a widely developed mid-crustal partial melt layer would account for e.g. the relatively flat topography of Tibet by decoupling the upper crust from the lower crust/upper mantle. Alsdorf et al. (1998) also use INDEPTH data, and interpret deep seismic reflection profiles to infer a partially molten, deformed layer below the Lhasa terrane, at depth of c. 12-18 km. They do not discuss the results in terms of mid-crustal flow, but do state that the shortening has been accompanied by melting of the middle crust and that, consequently, the weak middle crust accommodated much of the deformation. Unsworth et al. (2005) construct resistivity models from magnetotelluric data and interpret the low resistivity layer beneath Tibet to represent a zone of high fluid content.

Many of the above studies do not specifically conclude the existence of channel flow from the results, but the growing popularity of the mid-crustal channel flow theory in the past two decades has increasingly led to interpretation of many geophysical results from Himalayas and Tibet to specifically infer mid-crustal channel flow. For example, Chen et al. (2014) use the fan wavelet coherence method to estimate the variations in the total elastic thickness and anisotropy of the lithosphere in SE Tibet. They conclude that at least in SE Tibet, the whole lithosphere is weak and mechanically anisotropic, which they suggest to imply continuous deformation and, possibly, crustal flow. Another example is Bao et al. (2015) who use Rayleigh wave dispersion and receiver function analyses to image two low-velocity zones in SE Tibet, interpreting these as discrete mid-crustal flow channels that facilitate the clockwise rotation of crustal material in that region. Klemperer (2006) summarizes geophysical and geothermal data and literature from Himalayan-Tibetan system to infer that Poiseuille-type flow is occurring throughout much of southern Tibet.

The presence of melts and other fluids in the present Tibetan middle crust is, all in all, undisputable. The critical question is whether the partially molten crust capable of flowing *en masse* in the manner required by the mid-crustal channel flow theory? For the mid-crustal channel flow to operate, the melting needs to take place at the length and width scales of the theoretical mid-crustal channel(s) (thickness a few to c. 20 km, length in the order of 100 km). In addition, those melts need to be fairly homogeneously distributed *and* survive at time scales necessary for significant lateral transport of material to occur (in the order of a few Ma). The melt fraction, melt distribution, and melt longevity at the tempo-spatial scale of a mid-crustal channel are, in other words, the first-order controls on the bulk rheology and mechanical behaviour of the orogenic mid-crust, although the rheology also depends on many other factors (e.g. rock permeability, chemical composition of the phases, grain sizes of the solid phase, density of the melt, metamorphic reactions during melting, ambient temperature, presence of a volatile phase, pore fluid pressure of melt and other fluids, strain rate and differential stresses; e.g. Berger and Kalt, 1999; Renner et al., 2000). It is crucial for the mid-crustal channel flow theory that not only the larger accumulated melt volumes (sheets and plutons) but also the relatively small, fairly homogeneously distributed melt volumes (observed as migmatitic leucosomes at outcrop) remain as melts for sufficiently long time scales for the channel flow to operate. However, the longevity, volume, and spatial distribution of the melts at a channel scale (both in time and space) are still relatively poorly understood.

Various experimental studies exist on the rheology of partially molten rock, mostly with respect to upper mantle rheology, but also on granitic rocks and metapelites (e.g. Arzi, 1978; Kohlstedt, 1992; Vigneresse et al., 1996; Rosenberg and Handy, 2005; Rutter et al, 2006; Hashim et al., 2013). Also the mechanisms and consequences of melt extraction and segregation, and the effect of deformation and stress on melt extraction and on rheology, have attracted much attention (e.g. Kriegsman, 2001; Holtzman et al., 2003; Katz et al., 2006; Holtzman and Kohlstedt, 2007; Menegon et al., 2011). The extrapolation of the experiments and models to crustal scale is problematic. Field data suggest that partial melts tend to migrate and accumulate into plutons, dykes, and sheets rather than being relatively homogeneously distributed throughout the mid-crust, especially where the partially molten crust is undergoing active deformation (e.g. Holtzman et al., 2003; Bons et al., 2008; Diener et al., 2014). On the other hand, the common occurrence of migmatitic rocks in exposed orogenic middle crust suggests that not all melts are transported from their source and accumulated into larger bodies. All this means that, in terms of mid-crustal flow, the properties and behaviour of partially molten rocks at depth and at the scales of a mid-crustal channel are debated and the bulk viscosity estimations vary, often depending on which observation scale, modelling approach and/or flow law is used (e.g. Hilley et al., 2005).

It is undisputed that melts do weaken the rock. Two main rheological thresholds are found in partially molten, originally solid rocks. The first significant rheological threshold in deforming rocks containing melt is the ‘melt connectivity transition’, MCT, which occurs at a melt fraction (Φ) of ~5-8% (e.g. Vigneresse et al., 1996;

Rosenberg and Handy, 2005; although it should be noted here that solid rocks are weakened already from 400-600°C, prior to actual melting; e.g. Sygala et al., 2013). The next significant threshold is the 'solid-to-liquid transition', SLT, or 'rheologically critical melt percentage', where the solid (crystal) framework breaks down and the aggregate becomes entirely melt-supported, which occurs at Φ ~20-50%: the suggested SLT is highly variable depending on e.g. the modelling/experimental approach and technique, especially in terms of using a volatile phase to assist melting; whether the experiment/modelling is considering rocks crystallising out of magma rather than partially melting, originally solid rocks, as the original melt distribution in both cases are very different; and whether or not partial melt segregation due to e.g. active deformation is efficient, so that melt accumulates into lenses, pockets and/or layers of variable sizes (e.g. Arzi, 1978; Van der Molen and Paterson, 1979; Vigneresse et al., 1996; Holtzman et al., 2003; Hier-Majunder et al., 2006; Rosenberg and Handy, 2005; Rutter et al., 2006). The strength drop at SLT is about four to five orders of magnitude (e.g. Arzi, 1978); however, Rosenberg and Handy (2005) argue that the reduction of the bulk rheology at MCT is actually more significant than that at the SLT, because the absolute drop in the bulk rock strength is more significant at MCT. In their study, the bulk strength drops significantly by Φ of ~5-7% with respect to the maximum shear strength of the continental crust, by about 600 MPa (i.e. up to 90% of the original); in contrast, the absolute strength loss at SLT is in the order of <1 MPa.

Despite the fact that melting significantly reduces bulk rock strength, the key questions with respect to mid-crustal flow models remain unanswered: i) what are the larger-scale rheological effects of (small) melt fractions and what does the melt distribution need to be with respect to the other channel flow parameters (channel thickness, pressure gradient, and relative velocities) to enable flow; ii) how reliably can the rheological properties obtained from laboratory experiments and models be extrapolated to natural conditions at a scale of a mid-crustal partially molten layer; and iii) whether the necessary strength values/melt fractions and distributions can be maintained at the temporal and spatial scales of orogenic deformation. Part of the problem is the constraints of laboratory techniques to reproduce the large spatial and temporal scales and slow strain rates of orogenic processes (e.g. Paterson, 1987), and that no reliable flow law exists to extrapolate the experimental data and observed rheological properties to orogenic scales. There is also insufficient information about the behaviour of partially molten rocks at melt fractions below the SLT. It has been estimated that a *solid* mid-crustal rock typically shows non-Newtonian (power-law), plastic to viscous-plastic behaviours at geologically characteristic strain rates (in the order of 10^{-14} s^{-1}; e.g. Weijermars and Schmeling, 1986; Bürgmann and Dresen, 2008). Complete silicate melts and partial melts with melt fractions well above SLT, i.e. melt supported aggregates, are generally considered to show viscous, approximately linear Newtonian behaviour (e.g. Van der Molen and Paterson, 1979; Kohlstedt et al., 1995; Renner et al., 2000), although indications exist that at least some silicate melts can behave in a non-Newtonian manner in certain geologically realistic but high strain rates (e.g. Dingwell and Webb, 1989). The non-Newtonian behaviour becomes increasingly dominant even at lower strain rates as crystallinity increases, and it has been suggested that non-Newtonian behaviour becomes the norm below Φ ~50% as the rheology and the mechanical behaviour becomes controlled by the solid phase (e.g. Stevenson et al., 1996; Dell'Angelo & Tullis, 1998; Rutter et al., 2006; Caricchi et al., 2007; Lavallée et al., 2007). This also has implications to the flow geometry: for Poisuille flow, a non-Newtonian material would exhibit a more rigid channel core (a "plug") with more intensely deformed channel walls than would a Newtonian material (e.g. Grujic, 2006).

Despite the difficulties, many attempts have been made to quantify the bulk viscosity necessary for mid-crustal flow, and to estimate whether those viscosities can be realistically achieved within the orogenic crust. The necessary bulk effective viscosity of the middle crust to induce flow has been considered to be 10^{19} Pa·s or less (e.g. Beaumont et al., 2004), although it should be noted that this value is parameter-dependent: Beaumont et al. (2004) use channel parameters approximately corresponding to those in the Himalayan-Tibetan system. Most estimates of the *in situ* middle crustal viscosity vary from 10^{19} Pa·s (e.g. Block and Royden,1990) to 10^{18} Pa·s or less in regions of high heat flow (Bailey, 2001), to as low as 10^{16} Pa·s for "wet" quartz-rich deep crust (Wang et al., 1994). Whether any of these values can be realistically maintained at the tempo-spatial scales of an orogenic channel, is debated: e.g. Beaumont et al. (2004) only qualitatively state that a “small *in situ* component of partial melt” or “other processes” should suffice to gain the necessary viscosity for their channel parameters (set to correspond to the Himalayan-Tibetan system). Furthermore, it is very likely that the bulk rheology and other properties and, therefore, the mechanical behaviour of the mid-crust change significantly in space and time during the various stages of partial melting and orogenic deformation (e.g. Berger and Kalt, 1999). All in all, modelling mid-crustal flow is obviously a very complicated matter, and as long as the models and calculations make several assumptions that remain unproven, the results will continue to be debated.

WHAT MIGHT A PALAEOCHANNEL LOOK LIKE?

Various studies of exposed orogenic middle crust have been carried out to infer that mid-crustal channel flow once operated in those orogens. Outcrop studies attempting to address channel flow are challenging from the outset, especially in shield areas because their typically flat topography means that the outcrop patters are rarely 3D to any significant degree. In other words, a cross section view is usually effectively missing. In addition, even the advocates for the mid-channel crustal flow agree that the flow and, therefore, the resulting patterns will be more complicated than a simple Couette-Poiseuille scenario would expect, due to the variations in the flow type in time and space and to the rheological/lithological, structural, thermal, and other heterogeneities of the lithosphere; however, the complexity does not in itself present an argument against channel flow (e.g. Beaumont et al., 2004). Any resulting outcrop patterns cannot be expected to be nicely organised to reflect the flow. However, if flow occurred, the resulting patterns have to reflect that flow, although it is important to keep in mind that the inverse is not necessarily true, i.e. the channel flow might not be the only process that can explain the observed patterns. Below, I will discuss this statement in the light of field studies and 3D numerical modelling.

Numerical modelling of channel flow

Various 2D numerical models exist specifically for mid-crustal channel flow (e.g. Jamieson et al., 2011; Rey et al., 2011). Unfortunately, 3D numerical models do not yet exist for combined Couette-Poiseuille flow, which is the suggested flow mechanism within a mid-crustal channel. Pure Couette channel flow 3D models in viscous fluid do exist, and although they do not directly represent the mid-crustal channel flow where Poiseuille flow is a significant contributor, I will discuss Couette flow models here simply in order to demonstrate that various 3D geometries can result from even such a basic flow.

Gibson et al. (2009) investigate planar Couette flow patterns in a fairly high-aspect ratio channel (x:y:z = 8:1:8; for mid-crustal channels, the aspect ratios are likely to be even larger), of a fluid with a random initial internal organisation and relatively low Reynolds number of Re = 400 (Fig. 2; see also www.channelflow.org for videos of the flow models). The flow models show cyclic behaviour and that significant geometric changes can be expected in the flow patterns through the life span of the flow. The Reynolds number (Reynolds, 1883) gives the ratio between the inertial forces and viscous forces in a fluid, therefore quantifying which force is dominant and helping to assess the flow type. A Re of >2000 is normally needed for turbulent flow, for example, whereas Re < 2000 is normally dominantly laminar flow in low-aspect ratio channel ("pipe flow"); however, the flow type is highly dependent on factors such as the aspect ratio of the channel, or the channel wall roughness (Gibson et al. 2009 and references therein). The low Re = 400 in the Gibson et al. (2009) models is considered to be just below the turbulence threshold in their models with high aspect ratios. Re = 400 is an expression of a low-inertia, highly viscous fluid, but it is probably still too high for partially molten rocks (migmatites) as shown by a simplified calculation:

$$Re = \text{inertia/viscosity} = (D * d * v) / \mu$$

where D = Density, d = diameter of the channel, v = velocity of the flow, and μ = dynamic viscosity.

Geologically realistic parameters of D = 2800 kg/m^3, d = 134000 m (for a channel of e.g. 10 x 200 km, i.e. circumference c = 420 km, giving an average d = 2(c/2π), although the diameter of a high aspect ratio channel varies a lot), v = $6.34*10^{-10}$ m/s (i.e. 2 cm/year), and μ = 10^{19} Pa·s would give an extremely low Re = $2.4*10^{-20}$. Even changing the parameters drastically (but within geologically realistic boundaries) would not bring Re much higher, not even close to unity.

The very low inertia (expressed by the very low Re) for migmatites would effectively rule out any turbulence in the instantaneous flow pattern. The finite strain patterns that form during the long geological time scales at which the channel flow would operate are, therefore, a product of progressive deformation and the internal/local stress field variations within the channel rather than turbulence. The Gibson et al. (2009) models are, therefore, not used here as analogues for mid-crustal channel flow: they are only used to give a very simplified example of how different outcrop patterns may form under the same flow parameters, ahead of discussing actual outcrop patterns in the next chapter.

Figure 3 presents a simple thought exercise of the potential effect of Couette flow on initially horizontal vs. moderately (c. 35° towards east) tilted layers/foliation with respect to a horizontal upper and lower rigid plates on both sides of the channel in Figure 2. The implied structural geometries are purely based on the visual, qualitative estimation of how the relative orientation and magnitude ("force") of the flow in any given location within the modelled channel would affect the layers. The estimation assumes that the entire package behaves rheologically fairly homogeneously (except strain partitioning into shear zones) and responds to the modelled flow paths in a manner of approximately coherent viscous material. Note that the "shear zones" in the structural models are not likely to be discreet fault or shear planes, but diffuse zones of more intense deformation/higher strain rates.

The two simple thought exercises ignore important factors such as rheological heterogeneity within the channel and the development of any secondary foliation during flow, but demonstrate that already the simple factor of the pre-flow geometry of the layers/foliation has a significant impact on the resultant geometries. In structural model 1 (Fig. 3A), the originally sub-horizontal layers/foliation might produce dome-and-basin geometric patterns at outcrop, with the long axes of the domes approximately parallel to the direction of the flow, reflecting the "stream-wise streaks and rolls" of the flow that are in the model caused by the variations in the local flow directions and strengths (similar patterns, i.e. (elongate) domes in real rocks are probably not caused by the same process because any measure of turbulence is unlikely as discussed above; domes in real rocks usually result from local stress field and strain/flow type variations induced by the rheological differences and interactions between middle and upper crust; see the discussion chapter). The "east-west" fold axes in this model are doubly plunging. Additional folds may develop at high angles to the flow direction where local flow orientations converge, in which case some sheath/overturned folds with "north-south" fold axes might be expected (Fig. 3A, inset). The stretching and crenulation lineation trajectories are here assumed to mostly develop in the fold hinge orientations, and would, therefore, be gently plunging both E and W in the case of model 1. Additional stretching lineations would develop along the shear zones displacement vectors where the lineation plunges might be steeper depending on the shear zone kinematics, and possibly along the secondary "north-south" fold hinges as well (Fig. 3A; see also Chardon et al. (2009) for predicted foliation and lineation patterns for horizontal flow).

Model 2, where the geological layering/foliation is considered to have a pre-flow dip of c. 30-35° toward the upper plate motion direction ("east"), shows quite a different structural geometries compared to model 1 (Fig. 3B). The produced folds have moderately to fairly steeply "eastward" dipping axes and sub-vertical, "east-west" striking axial planes. In addition, another fold orientation would seem to develop, with fold axes that are highly oblique to the transport direction (i.e. "north-south") and "east"-verging to sub-horizontal axial planes; these can presumably develop into sheath folds as the flow progresses (Fig. 3B, inset). The stretching and crenulation lineations trajectories dominantly follow the "eastward" plunging fold axes and the shear zones displacement vectors and can be moderately to fairly steeply plunging, although some lineations could well form along the "north-south" fold axes as well (Fig. 3B).

Mineral lineations of elongate minerals might be also expected within the rock volume as minerals rotate towards the x-axis of the local strain ellipsoid. These lineations would probably vary significantly in both models, depending on the relative motion of the flow (i.e. the local orientation of the strain ellipsoid) in a particular location. The wavelengths of the major folds are in the order of c. 10 km, mostly reflecting the spatial distribution of the “disturbances” in this model. The shear zones are mostly flow-parallel to slightly oblique (forming where internal flows in opposite directions move "past" each other) and can show a variety of displacement styles from dip-slip, to oblique-reverse or oblique-normal, to strike-slip. The shear zones do not seem to develop a consistent conjugate pattern as would be expected for a stationary, Andersonian stress field: the rotational component caused by the relative shearing of the upper and lower plates seems to favour flow-parallel shear zones with variable kinematics instead. The locations and kinematics of the shear zones are estimated purely from the relative 3D flow directions in the model and are, therefore, the same for both models.

This thought exercise is rudimentary, but its aim is to illustrate how even a simple change in the initial geometries with respect to the channel boundaries results in very different outcrop patterns for structures within a crustal channel. Therefore, there is no single "typical" outcrop pattern of internal channel structures, which means, inversely, that outcrop patterns alone probably cannot used as an evidence for channel flow. The final channel-internal structural patterns would, naturally, be further complicated by continued shearing and flow, and by the presence of significant pre-existing lithological (rheological) and structural heterogeneities. Furthermore, as elaborated by e.g. Miller et al. (2006), outcrop structures such lineation, foliation, and asymmetric fabrics can record boundary conditions reflecting orogen-scale flow, local heterogeneous deformation and strain partitioning, or a combination of these and can also change through time as the orogen evolves. The difficulty in defining a "typical" internal structure for a mid-crustal channel is further illustrated by the examples presented in the next chapters.

Examples from outcrop studies

Several conditions need to be met for outcrop studies and field data looking at potential mid-crustal flow patterns. Firstly, the scale of observation needs to be large enough to account for the scale of the putative palaeochannel. The mid-crustal channel theory expects that any mid-crustal channel should be several km in thickness (estimated 10-20 km in the Tibetan-Himalayan system; e.g. Clark and Royden, 2000; Beaumont et al., 2004), and possess a lateral width along the orogenic strike of at least a couple of hundreds of km, potentially significantly more. In practice this probably means a data collection from a field area of preferably at least several hundreds of km^2. Secondly, the overall kinematics, geometries, and other data should agree with the expected first-order characteristics suggested for a mid-crustal channel (such as the coeval movement on shear zones with opposite kinematics bounding the channel; e.g.

Godin et al., 2006). In outcrop studies of high metamorphic grade rocks, the syn-peak temperature kinematics are not usually easily constrained because recrystallisation processes operate very efficiently at high temperatures, often destroying any obvious fabric asymmetries, although microanalytical methods might reveal the original grain shapes in ideal circumstances (e.g. Jessell et al., 2003). Retrograde, post-peak temperature deformation fabrics may or may not result from the same stress field as the syn-peak deformation. Stretching, crenulation, and mineral lineations together with (large-scale) folding patterns of especially asymmetric folds probably provide the most reliable kinematic controls. Stretching lineations might be strongest in shear zones and along fold hinge lines, especially if the folds are shear or sheath folds. However, it should be noted here that the stretching lineations will also be easily affected by recrystallisation processes, and that purely geometric consideration of structural asymmetries can also be risky because strain partitioning at various scales lead to non-uniqueness of many asymmetric structures (e.g. Carreras et al., 2013). Foliation patterns are also often useful for determining local deformation kinematics but, again, the final large-scale foliation patterns might be highly affected by strain partitioning, and by their pre-deformation geometries, as was also seen in the thought exercise in Fig. 3.

Examples of outcrop patterns suggested to have formed by mid-crustal channel flow, as defined in this paper, are presented in Fig. 4, and others that show similar outcrop patterns but are interpreted to have formed by other tectonic mechanisms are shown in Fig. 5. In terms of examples of pro-flow studies, Hatcher & Merschat (2006; Fig. 4A) suggest a "tectonically forced orogenic strike-parallel channel" in the Appalachians, based largely on the foliation and lineation patterns observed on a large area. Cagnard et al. (2006) similarly use regional patterns of migmatitic and syn-orogenic granitoid foliation and stretching lineations to infer mid-crustal channel flow in the Palaeoproterozoic Svecofennides in Finland (Fig. 4B). A third example comes from Trans-North China Orogen, where Trap et al. (2011; Fig 4C) suggest mostly lateral channel flow, again based mainly on foliation and lineation patterns (although they also suggest some diapirism took place with uprising of low density partially-molten and magmatic rocks). There are many similarities in all examples, such as all (migmatitic) foliations being mostly gently to moderately dipping. However, striking differences exist. The outcrop patterns are quite different in terms of the relationships between the observed foliations and lineations. In the Appalachian example (Fig. 4A), the stretching lineations define an arcuate pattern and are shallowly plunging, while the mostly moderately dipping foliations are lobate/irregular (except within the Brevard fault zone) but dip mostly toward the SE. In southern Finland (Fig. 4B) the regional lineation pattern is fairly straight although some scattering is indicated in the stereographic projections, the lineations are shallow to steeply plunging in opposite directions, while the dominantly moderately dipping foliations define dome- or lens-like features (except in shear zones where both foliations and lineations are steeper; see also e.g. Ehlers et al. 1993, for the regional migmatitic foliation patterns). In Trans-North China Orogen (Fig. 4C), the lineations are also of constant orientation to somewhat scattered but shallowly to moderately dipping throughout; the foliation traces define km-scale folds on the map and in stereographic projections for S2 (the inferred fold axes of which are approximately parallel with the majority of the lineations); and the cross-section shows that the folds are related to dome-like features at depth, with a normal-sense shear zone at its northern flank. The interpretations also vary, from flow in an orogen-frontal (Himalayan) type of a mid-crustal channel in Fig. 4A; to East Tibetan mid-crustal type of lateral (here westward) channel flow in Fig. 4B; to both E and W directed channel flow (but with interpreted overall eastward extrusion of the middle crust) in Fig. 4C.

Similar structural (foliation/fold) patterns to those presented in Fig. 4, but interpreted by the authors to *not* represent channel flow in the ductile middle and lower crust, are shown in Fig. 5. The type of orogen in some of these examples is different from the Tibetan-Himalayan system, but the point here is to show examples of how the patterns in Fig. 4 might be formed in alternative ways. In Fig. 5A (Ridley, 1982), although the studied exposure is at a smaller scale than Fig. 4A, the patterns are similar when extrapolated to the scale of Fig. 4A: arcuate stretching lineations and variable foliation trends. However, here the patterns are interpreted to have formed due to thrust displacement of a ductile lower crustal sheet during subhorizontal shearing rather than channel flow, so that the lineations and fold hinge lines are rotated toward the edge of the thrust sheet during progressive deformation. In Fig. 5B (Chardon et al., 2009, 2011), the gently plunging lineation trends are fairly straight, and the gently to moderately dipping foliations define dome- or lens-like structures, similarly to Fig. 4B. The pattern is explained by “lateral constrictional flow” (LCF), rather than channel flow: in the LCF model, the orogen-parallel, syn-convergence escape is facilitated by a network of shear zones and constrictional, orogen-parallel stretching in the viscous middle crust that may be either decoupled from or coupled with both the upper and/or the lower crust (see also Culshaw et al., 2006 about discussion on the upper-middle crustal coupling). The steep lineations present in Fig. 4B are absent in Fig. 5B, which may mean that the lineation patterns in Fig. 4B include some deformation zones that were not recognised in the field due to the often diffuse nature of high-grade shear zones; on the other hand, the model 2) in Fig. 5B predicts that stretching lineations may not be gently dipping everywhere, especially if the upper and middle crust are (partially) coupled (see also e.g. Tikoff and Greene, 1997). The final example in Fig. 5C (Denèle et al., 2007) is analogous to Fig. 4C, showing gently dipping, relatively straight, doubly plunging stretching lineations, and foliation patterns defining km-scale folds along an elongate, dome-like feature. The lineation patterns are explained by early (but post-thickening) top-to-east subhorizontal, syn-transpressional shearing of the upper crust, the folds having subsequently formed during the progressing transpression. Although the patterns shown in Fig. 5C are for a local feature (the Hospitalet Massif), the scale of the folding patterns is similar as in the high-pressure belt HPB of the Trans-North China Orogen in Fig. 4C. Furthermore, the authors note various other areas within the Axial Zone of the Pyrenees that display similar patterns to the Hospitalet Massif (such as the migmatitic Aston Massif directly to the north), and the Axial Zone as a whole is of a similar scale as the HPB.

An example from southwestern Finland

Figure 6 shows a simplified geological and structural map from the Turku archipelago, southwestern Finland, compiled from published geological maps and new field data collected by the author. In southern Finland, the migmatitic middle and lower crust of the Palaeoproterozoic Svecofennian orogen is exposed. The structural history of the southern and southwestern Finland is complicated, but in essence an early, (apparent) NE-SW compression produced tight to isoclinal, originally probably mostly recumbent F1 folds (e.g. Ehlers et al., 1993). A c. 20 Ma long period of relative tectonic quiescence followed, with thermal relaxation and intraorogenic basin development (e.g. Bergman et al., 2008). Some migmatitic melts are associated with F1, but the most voluminous anatexis occurred just before and partly during the next folding event F2 (e.g. Ehlers et al., 1993; Skyttä and Mänttäri, 2008). During this wide-spread anatexis, the partially molten crustal package was subjected to gravitational spreading/escape/flow, the details of which are still unclear (Skyttä and Mänttäri, 2008; Torvela et al., 2013). The microcline granite "sheets" in Figure 6 were formed at this stage and most of them show moderate to strong internal deformation, being folded by the F2 folds (e.g. Ehlers et al., 1993; Skyttä and Mänttäri, 2008). The F2 event formed open, mostly upright folds, with approximately E-W striking axial planes, refolding the F1 folds and the spreading/collapse structures, and producing an overall Type 3 fold interference pattern with the F1 folds (Ramsay, 1962). A final folding stage F3 with approximately perpendicular (i.e. apparently E-W directed) compression finally deformed the F1-2 and the spreading/collapse patterns in a Type 2 fold interference style (Ramsay, 1962): this event formed gentle, crustal-scale folds with N-S trending axial planes, forming and/or enhancing the dome-and-basin structure seen today (e.g. Lahtinen et al., 2005). The various interference patterns can be seen on geological maps and some are obvious also in the simplified Figure 6. No migmatites are associated with the F3 folds.

The F1 folds in the area of Figure 6 generally have relatively shallow (<40°), mostly eastward plunging fold axes that in the map area are almost exclusively preserved along the ~E-W striking F2 fold limbs. The F2 fold axes are dominantly E plunging, usually by 40-70°, with a mean orientation of c. 095/55 which is very close to the β direction predicted by the migmatitic foliations. Two eastward plunging F2 anticlines dominate the map area, separated by the Rosala-Jurmo zone (RJZ). The migmatite granite bodies/sheets follow approximately the S1 lithologies that were folded during the F2 event. The granites seem to be "squeezed" into the anticline crests, away from the synclines and from the steeply dipping fold limbs. As a result, the synclines are very tight (RJZ is interpreted here to be one such syncline rather than a shear zone) whereas the anticlines show more open morphologies. Note that, although significant exceptions do exist, the microcline granite "sheets" in southern Finland are not homogeneous but contain significant volumes of protolith/migmatitic host rock: the microcline granite areas are traditionally defined as areas where approximately >50% of the rock volume consists of granitic material, as opposed to other migmatitic areas with approximately <50% microcline granite. The rock type contacts are, therefore, very diffuse in reality. In the area of Figure 6, the microcline granites are intermixed with migmatitic schists and granitoids, containing approximately between 50-80% granitic material.

Observed lineations are mostly stretching, mineral, and crenulation lineations. On average, the lineations follow the fold axial plane and are almost parallel with the average F2 fold axis trend (but shallower, by about 10°). In places, remnant L1 lineations can be seen as they are folded by F2 (omitted from the map for clarity), and some steeply southward plunging stretching lineations are associated with subvertical constriction induced by the apparent N-S compression (also omitted from the map for clarity); but in general the lineations in the area are E-plunging crenulation and F2 fold axis-parallel stretching lineations, outlining relatively straight, approximately E-W trajectories on the map. E-plunging lineations are also prominent within the E-W striking zones along the fold limbs (most notably the RJZ), although the E-W zones also often show W-plunging lineations, probably as a result of relative movements of the folded domains and/or the migmatitic granites during deformation. The geometric relationships, in summary, indicate that the E-W lineations formed during the F2 folding event. It is unclear whether the present eastward plunge of the fold axes and the lineations is an original feature, or whether there was a later eastward tilting of the crust; however, significant tilting such as required in this case has not been reported for southern Finland.

The foliation-lineation-fold relationships for the D2 event are much like those interpreted to represent mid-crustal channel flow in Figures 4B and 4C. There is also much resemblance to the expected geometries presented in the thought exercise in Figure 3B. At the same time, the relationships are almost identical to those observed in Figure 5C, and bear much resemblance to Figure 5B as well; these are field examples that do not infer channel flow. In summary, although the area in Figure 6 might be interpreted as an example of a palaeochannel based on the internal geometric relationships, an equally likely explanation is probably a combined (eastward) shearing and/or doming/folding model such as presented for the Hospitalet Massif in Figure 5C, for example. A further complication is that in southern Finland, similarly for many other shield areas with exposed mid-crust, the first-order relationships required for a mid-crustal channel (e.g. coeval bounding shear zones with opposite shear senses; Godin et al., 2006) are very difficult or impossible to affirm: erosion and/or later deformation processes have removed or obscured the putative channel boundaries, so that, if they can be found at all, their characteristics cannot be established with certainty.

DISCUSSION

The first-order characteristics of a mid-crustal channel (e.g. coeval bounding shear zones with opposite shear senses; Godin et al., 2008) set the boundary conditions for channel flow. However, it should be noted in this context that the uniqueness of these first-order characteristics have also been contested: e.g. Jones et al. (2006) note that at least some of the first-order field relationships predicted for channel flow can also be produced by transpression and related crustal stretching/constriction and that the relationships are, therefore, non-unique. In this paper, I have not considered these first-order boundary conditions, because many field examples used to study deformation in the mid-crust come from deeply eroded shield and other areas where the channel boundaries, if they existed, cannot be observed. Instead, I have focussed on demonstrating the non-uniqueness of the internal structures and geometries of a putative mid-crustal channel. From the examples in this paper, it is clear that a variety structural geometries can potentially form where and if mid-crustal channel flow occurs, but similar geometries might also result from other crustal-scale mechanisms that do not necessarily require *channel* flow to operate. Below, I briefly discuss further what are probably the most important of these alternative mechanisms: doming, and orogenic spreading/escape through constriction and/or shearing in the middle crust.

Various studies exist on gneiss domes, i.e. dome-formed bodies of high-grade, commonly migmatitic gneisses resulting from vertical mid- and lower crustal material redistribution: e.g. Whitney et al. (2004) give a good overview of gneiss domes; Platt et al. (2015) discuss gneiss domes in the wider context of metamorphic core complexes (MCCs); Rey et al. (2009) model how partial melts and extension rates influence the development of MCCs; and Le Pourhiet et al. (2012) show how the kinematics of MCC development significantly influences the resulting internal structural (foliation-lineation) relationships. Doming does not, of course, exclude channel flow as such: if mid-crustal channel flow, as defined in this paper, does occur, doming is probably an important aspect of channel flow, as seen from the various examples, and as discussed by e.g. Whitney et al., 2004 who describe the relationships between horizontal flow and vertical diapiric flow in dome formation (Fig. 7A; see also e.g. Beaumont et al., 2004). However, although a local lateral component to the mid-crustal movements must occur in the context of diapiric gneiss domes, the extent of that lateral flow at an orogenic scale (i.e. existence of channel flow) is open to debate.

Platt et al. (2015) note that the vertical material transport in developing domes can be driven either "actively" by buoyancy forces, or "passively" by isostatic forces (e.g. due to upper crustal extension), or by a combination of these. The experiments by Harris et al. (2012) also show that domes can form "passively" in contraction, much like suggested by Denele et al. (2007) for the Hospitalet dome (Fig. 4C). It should perhaps be noted here that Harris et al. (2012) interpret their experiments results to support the orogen-frontal extrusion channel model, but the results could also be used to infer that an extrusion channel is probably not necessary for the fold and dome structures to form. Whitney et al. (2004) note that the major difference between channel flow and diapiric flow should be seen in each case in the PT, Tt, and PTt paths (Fig. 7A). However, although the expected PTt paths for lateral vs. vertical flow are different at depth, once the rocks are exposed at the surface, even those that have possibly undergone channel flow at some point will have experienced P and T reduction and associated retrogression (see also Jamieson et al., 2004, 2006; Grujic et al. 2011), probably rendering it impossible to distinguish the PTt paths from each other (especially in older orogens where the age determination errors are often too large to allow a sufficiently accurate reconstruction of events).

In terms of field structural data, Whitney et al. (2004) observe that very careful analysis of foliation patterns and, in particular, lineation trajectories are required, and ideally diapiric domes should display specific features such as radial lineations and flattening or constriction at particular localities; however, these are easily distorted/ overprinted during progressive crustal deformation (see also e.g. Chardon et al. (2009) for predicted foliation and lineation patterns for horizontal vs. vertical flow, and Le Pourhiet et al. (2012) on how the mode and kinematics of crustal deformation that control the dome formation affect foliation-lineation relationships). E.g. Platt et al. (2015) note that diapir flow-dominated domes should have steep or even overturned margins, although numerical modelling work by e.g. Rey et al. (2011; Fig. 7A) and Whitney et al. (2013) shows that this is not always the case, especially at the early stages of the dome development or if the deformation rate is slow. On the other hand, “passive” domes as defined above do not necessarily show steep margins (e.g. Platt et al., 2015). Margin geometries are certainly very useful for gneiss dome recognition where the relationships between the more rigid upper crust and the migmatitic middle crust can be relatively easily observed. However, many inferred channel flow examples come from old, eroded orogenic roots where the depth dimension of outcrop studies is limited, the middle-upper crustal relationships cannot be observed anymore, and there is often significant uncertainty as to exactly which crustal level is observed (both in real palaeodepth and in terms of regional and even local crustal structure). Further complications are induced by progressive deformation and possible later orogenic and/or extensional phases: these often result in crustal tilting and structural overprinting that obscure the original structures, and in metamorphic reactions that may sometimes completely erase the previous PTt signature. The numerical model predictions in Figure 7A illustrate the point: depending on the crustal level and the “intensity” of doming, the observed structures would be very different and especially the deep dome structures might indeed be interpreted to represent mid-crustal channel flow. Fig. 7A also shows that well-defined detachments that typify many gneiss domes at higher crustal levels (e.g. Platt et al., 2015) are unlikely to form well within the ductile/partially molten regime; if only this crustal level is exposed, as is the case in many older orogens, it will be impossible to with certainty determine the upper-middle crustal structural and kinematic relationships. The same of course goes for the first-order boundary conditions of a mid-crustal channel: if only a deep crustal level is exposed, the boundary conditions are impossible to constrain.

The summary is that, despite careful field data collection and analysis, it can be very difficult to constrain the exact relationships between foliation, folding, and lineation patterns (even with the help of age determination and geothermobarometric data) in order to determine how much lateral (channel) flow vs. vertical flow ("active" or "passive" doming), took place. Lateral channel flow and doming-related vertical flow are linked: the channel flow model does predict doming (e.g. Beaumont et al., 2004; see also Fig. 3A), and local lateral flow is needed to redistribute and transport the material into the diapir, but the point here is that doming (and orogenic spreading/collapse) may not require channel flow at a crustal scale (see also Vanderhaeghe and Teyssier, 2001b). Doming in itself is, in other words, not exclusive evidence for channel flow.

In terms of how lateral orogenic spreading and escape are accommodated, the most important alternative model to mid-crustal channel flow is probably the "lateral constrictional flow model" (LCF; Fig. 5B; Chardon et al., 2009, 2011). The LCF model invokes a network of shear zones and constrictional, mostly orogen-parallel stretching in the viscous lower crust. On the other hand, the existnece of shear zones is not an argument against channel flow: Couette-Poiseuille type mid-crustal channel flow would also lead to a development of shear zones that help to accommodate material transport. Probably the main and the most fundamental difference between the channel flow model and the LCF model is that the LCF model does not require material to move *en masse* for long distances along a mid-crustal channel. Instead, although some lateral movement or flow of material would occur in LCF due to a combination of local melt accumulation/transport and constrictional deformation, the bulk of the spreading is essentially accommodated by both vertical and inclined shear planes and movements of crustal "blocks" with respect to each other, and by vertical flattening (producing the flat foliations within the crustal "blocks" at depth; Fig. 5B). The LCF model, like the channel flow model, does rely on the existence of a weak middle/lower crust, but the viscosity probably need not be as low nor as homogeneously distributed as for the channel flow model, and the upper-middle-lower crust rheological contrasts do not need to be as large. The LCF also explains the very common sigmoidal shear zone patterns defining asymmetric, lens-shaped "blocks" of less deformed rocks, a feature observed in many exposed roots of hot and ultrahot orogens (see also Fig. 4B where such a shear zone pattern can be observed in southern Finland). A sigmoidal shear zone pattern might be more difficult to explain with channel flow theory, even if channel flow is expected to form shear zones approximately parallel to the flow direction (Fig. 3). The LCF model works during the orogenic compression/transpression, although the resulting structures can be partly extensional/transtensional and produce flattening structures (Fig.5; Chardon et al., 2009, 2011).

In detail, the LCF model does not contradict the other suggested mechanisms in Figure 5: the flattening/extensional component of the LCF allows the formation of subhorizontal shearing as suggested for the Hospitalet Dome (Fig. 5C) and the thrust stacking in suggested for Syros (Fig. 5A). The model also allows formation of gneiss domes, especially if the upper and middle crust are coupled. It can explain all the geometries observed in Figure 6 as well. Recent seismic reflection studies have given some support to the LCF model in that networks of shear zones do seem to play an important role in the strain accommodation of the mid-crust (Fig. 7B): Torvela et al. (2013) identified extensional shear patterns in the exposed orogenic roots of the Svecofennian orogen (in a study area c. 100 km NE from the Jurmo-Rosala area in Fig. 6), while Wang et al. (2011) have interpreted networks of thrusts and strike-slip shear zones in a reflection seismic study from northeastern Tibet. Both shear zone types are predicted by Chardon et al. (2011).

As a final note, LCF-type escape (but also channel flow) and orogenic lithospheric thickening can be seen as competing processes: both the extensional/transtensional processes of the LCF model and channel flow will result in thinning of the middle crust, while simultaneous orogenic convergence will induce thickening, although this would require a complete decoupling between the upper and middle crust. The relative rates and extents of these processes play a role in determining whether the orogenic plateau of a hot orogen (like Tibet) is rising, stable, or collapsing. Recent results suggest that the Tibetan crust is indeed thinning (Ge et al., accepted); whether this is accommodated by LCF-type escape, by channel flow, by a combination of these, and/or by some other mechanism, remains unanswered.

Summary

This paper shows examples of the variability of outcrop patterns that have been inferred to result from mid-crustal channel flow, but also examples of the non-unique nature of those patterns. As a conclusion, it is very unlikely that Couette-

Poiseuille type mid-crustal channel flow, if it exists, can be reliably interpreted from outcrop data, especially if the putative channel boundary kinematics and properties cannot be observed. The general feasibility of the mid-crustal channel flow is also discussed: while its existence remains an open question, the processes and structures (outcrop patterns) in the Himalayas, Tibet, and exposed old orogenic roots can also be explained by other, perhaps simpler, mechanisms. The main challenge of the Couette-Poiseuille type mid-crustal channel flow is probably the need to maintain the appropriate bulk physical conditions at very large tempo-spatial scales within the crust. A strong contestant is the lateral constrictional flow model by Chardon et al. (2009, 2011): the various phenomena and patterns of shear zone networks, foliation-lineation relationships, and gneiss dome formations can be explained by it, while it is less restrictive in terms of the required rheological mid-crustal bulk properties.

Acknowledgements

Åbo Akademi University (Geology and Mineralogy) is sincerely thanked for financing the field work in the Finnish archipelago, and Carl Ehlers for the discussions and advice. The constructive and detailed reviews of Djordje Grujic and John Platt are gratefully acknowledged, and the editors Rick Law and Ryan Thigpen are thanked for their comments and effort.

REFERENCES

Alsdorf, D., Brown, L., Nelson, K.D., Makovsky, Y., Klemperer, S., and Zhao, W., 1998. Crustal deformation of the Lhasa terrane, Tibet plateau from Project INDEPTH deep seismic reflection profiles. Tectonics, v. 17, p. 501-519.

Anczkiewicz, R., Chakraborty, S., Dasgupta, S., Mukhopadhyay, D., Koltonik, K., 2014. Timing, duration and inversion of prograde Barrovian metamorphism constrained by high resolution Lu-Hf garnet dating: A case study from the Sikkim Himalaya, NE India. Earth and Planetary Science Letters, v. 407, p. 70-81.

Arzi, A., 1978. Critical phenomena in the rheology of partially melted rocks. Tectonophysics, v. 44, p. 173-184.

Bai, D., Unsworth, M.J., Meju, M.A., Ma, X., Teng, J., Kong, X., Sun, Y., Sun, J., Wang, L., Jiang, C., Zhao, C., Xiao, P., and Liu, M., 2010. Crustal deformation of the eastern Tibetan Plateau revealed by magnetotelluric imaging. Nature Geoscience, v. 3, p. 358–362.

Bailey, R.C., 2001. Dynamical analysis of continental overflow. Journal of Geodynamics, v. 31, p. 293-310.

Bao, X., Sun, X., Xu, M., Eaton, D.W., Song, X., Wang, L., Ding, Z., Mi, N., Li, H., Yu, D., Huang, Z., and Wang, P., 2015. Two crustal low-velocity channels beneath SE Tibet revealed by joint inversion of Rayleigh wave dispersion and receiver functions. Earth and Planetary Science Letters, v. 415, p. 16-24.

Beaumont, C., Jamieson, R.A., Nguyen, M.H., and Lee B., 2001. Himalayan tectonics explained by extrusion of a low-viscosity crustal channel coupled to focused surface denudation. Nature, v. 414, p. 738-742.

Beaumont C., Jamieson, R.A., Nguyen M.H., and Medvedev S., 2004. Crustal channel flows: 1. Numerical models with applications to the tectonics of the Himalayan-Tibetan orogen. Journal of Geophysical Research, v. 109, B06406, doi:10.1029/2003JB002809.

Berger, A., and Kalt, A., 1999. Structures and melt fractions as indicators of rheology in cordierite-bearing migmatites of the Bayerische Wald, (Variscan Belt, Germany). Journal of Petrology, v. 40, p. 1699-1719.

Bergman, S., Högdahl, K., Nironen, M., Ogenhall, E., Sjöström, H., Lundqvist, L., and Lahtinen, R., 2008. Timing of Palaeoproterozoic intra-orogenic sedimentation in the central Fennoscandian Shield; evidence from detrital zircon in metasandstone. Precambrian Research, v. 161, p. 231-249.

Bird, P., 1991. Lateral extrusion of lower crust from under higher topography, in the isostatic limit. Journal of Geophysical Research, v. 96, p. 10275-10286.

Block, L. and Royden, L.H., 1990. Core complex geometries and regional scale-flow in the lower crust. Tectonics, v. 9, p. 557-567.

Bons, P.D., Druguet, E., Castaño, L.-M., and Elburg, M.A., 2008. Finding what is now not there anymore: Recognizing missing fluid and magma volumes. Geology, v. 36, p. 851-854.

Bürgmann, R., and Dresen, G., 2008. Rheology of the crust and upper mantle: evidence from rock mechanics, geodesy, and field observations. Annual Review of Earth and Planetary Sciences, v. 36, p. 531-567.

Cagnard, F., Durrieu, N., Gapais, D., Brun, J.-P., and Ehlers, C., 2006. Crustal thickening and lateral flow during compression of hot lithospheres, with particular reference to Precambrian times. Terra Nova, v. 18, p. 72-78.

Caricchi, L., Burlini, L., Ulmer, P., Gerya, T., Vassalli, M., and Papale, P., 2007. Non-Newtonian rheology of crystal-bearing magmas and implications for magma ascent dynamics. Earth and Planetary Science Letters, v. 264, p. 402-419.

Carreras, J., Cosgrove, J.W., and Druguet, E., 2013. Strain partitioning in banded and/or anisotropic rocks: Implications for inferring tectonic regimes. Journal of Structural Geology, v. 50, p. 7-21.

Chardon, D., Gapais, D., and Cagnard, F., 2009. Flow of ultra-hot orogens: A view from the Precambrian, clues for the Phanerozoic. Tectonophysics, v. 477, p. 105-118.

Chardon, D., Jayananda, M., and Paucat, J.-J., 2011. Lateral constructional flow of hot orogenic crust: insights from the Neoarchean of south India, geological and geophysical implications for orogenic plateaux. Geochemistry, Geophysics, Geosystems, v. 12, Q02005, doi:10.1029/2010GC003398.

Chen B., Liu, J., Kaban, M.K., Sun, Y., Chen, C., and Du, J., 2014. Elastic thickness, mechanical anisotropy and deformation of the southeastern Tibetan Plateau. Tectonophysics, v. 637, p. 45-56.

Clark, M.K., and Royden, L.H., 2000. Topographic ooze: Building the eastern margin of Tibet by lower crustal flow. Geology, v. 28, p. 703-706.

Culshaw, N.G., Beaumont, C., and Jamieson, R.A., 2009. The orogenic superstructure-infrastructure concept: Revisited, quantified, and revived. Geology, v. 34, p. 733-736.

Dasgupta, S., Ganguly, J., and Neogi, S., 2004. Inverted metamorphic sequence in the Sikkim Himalayas: crystallization history, *P–T* gradient and implications. Journal of Metamorphic Geology, v. 22, p. 395–412.

Dell'Angelo, L.N., and Tullis, J., 1998. Experimental deformation of partially melted granitic aggregates. Journal of Metamorphic Geology, v. 6, p. 495-515.

Denèle, Y., Olivier, P., Gleizes, G., and Barbey, P., 2007. The Hospitalet gneiss dome (Pyrenees) revisited: lateral flow during Variscan transpression in the middle crust. Terra Nova, v., 19, p. 445-453.

Diener, J.F.A., White, R.W., and Hudson, T.J.M., 2014. Melt production, redistribution and accumulation in mid-crustal source rocks, with implications for crustal-scale melt transfer. Lithos, v. 200-201, p. 212-225.

Dingwell, D.B., and Webb, S.L., 1989. Structural relaxation in silicate melts and non-Newtonian melt rheology in geologic processes. Physics and Chemistry of Minerals, v. 16, p. 508-516.

Edelman, N.,1954. Geological map of Finland, Pre-Quaternary Rocks, sheet 1033 (Nötö), 1:100000. Geological Survey of Finland.

Edelman, N.,1973. Geological map of Finland, Pre-Quaternary Rocks, sheet 1034 (Nagu), 1:100000. Geological Survey of Finland.

Ehlers, C., Lindroos, A., and Selonen, O., 1993. The late Svecofennian granite–migmatite zone of southern Finland — a belt of transpressive deformation and granite emplacement. Precambrian Research, v. 64, p. 295–309.

England, P. & Houseman, G., 1989. Extension during continental convergence, with application to the Tibetan Plateau. Journal of Geophysical Research, v. 94, p. 17561-17579.

Francheteau J., Jaupart, C., Jie, S. X., Wen-Hua, K., De-Lu, L., Jia-Chi, B., Hung-Pin, W., and Hsia-Yeu D., 1984. High heat flow in southern Tibet. Nature, v. 307, p. 32- 36.

Gao, R., Wang, H., Yin, A., Dong, S., Kuang, Z. Zuza, A.V., Li, W., and Xiong, X., 2013. Tectonic development of the northeastern Tibetan Plateau as constrained by high-resolution deep seismic-reflection data. Lithosphere, v. 5, p. 555-574.

Ge, W.-P., Molnar, P., Shen, Z.-K., and Li, Q., accepted. Present-day crustal thinning in the southern and northern Tibetan Plateau revealed by GPS measurements. Geophysical Research Letters, doi: 10.1002/2015GL064347.

Gibson, J.F., Halcrow, J., and Cvitanović, P., 2008. Visualizing the geometry of state space in plane Couette flow. Journal of Fluid Mechanics, v. 611, p. 107-130.

Gibson, J.F., Halcrow, J., and Cvitanović, P., 2009. Equilibrium and traveling-wave solutions of plane Couette flow. Journal of Fluid Mechanics, v. 638, p. 243-266.

Godin, L., Grujic, D., Law, R.D., and Searle, M.P., 2006. Channel flow, ductile extrusion and exhumation in continental collision zones: an introduction. In: Law, R.D., Searle, M.P. and Godin, L. (eds.) Channel Flow, Ductile Extrusion and Exhumation in Continental Collision Zones. Geological Society of London, Special Publications, v. 268, p. 1-23.

Goscombe, B., and Hand, M., 2000. Contrasting P-T paths in the Eastern Himalaya, Nepal: inverted isograds in a paired metamorphic mountain belt. Journal of Petrology, v., 41, p. 1673-1719.

Grasemann, B., Fritz, H., and Vannay, J.-C., 1999. Quantitative kinematic flow analysis from the Main Central Thrust Zone (NW-Himalaya, India): implications for a decelerating strain path and the extrusion of orogenic wedges. Journal of Structural Geology, v. 21, p. 837-853.

Grujic, D., Casey, M., Davidson, C., Hollister, L.S., Kündig, R., Pavlis, T., and Schmid, S., 1996. Ductile extrusion of the Higher Himalayan Crystalline in Bhutan: evidence from quartz microfabrics. Tectonophysics, v. 260, p. 21-43.

Grujic, D., Hollister, L.S., and Parrish, R.R., 2002. Himalayan metamorphic sequence as an orogenic channel: insights from Bhutan. Earth and Planetary Science Letters. V., 198, p. 177-191.

Grujic, D., 2006. Channel flow and continental collision tectonics: an overview. In: Law, R.D., Searle, M.P. & Godin, L. (eds.) Channel Flow, Ductile Extrusion and Exhumation in Continental Collision Zones. Geological Society of London, Special Publications, v. 268, p. 1-23.

Grujic, D., Warren, C.J., and Wooden, J.L., 2011. Rapid synconvergent exhumation of Miocene-aged lower orogenic crust in the eastern Himalaya. Lithosphere, v. 3, p. 346-366.

Harris, L. B., Yakymchuk, C., and Godin, L., 2012. Implications of centrifuge simulations of channel flow for opening out or destruction of folds. Tectonophysics, v. 526-529, p. 67-87.

Hashim, L., Gaillard, F., Champallier, R., Le Breton, N., Arbaret, L., and Scaillet, B., 2013. Experimental assessment of the relationships between electrical resistivity, crustal melting, and strain localization beneath the Himalayan-Tibetan Belt. Earth and Planetary Science Letters, v. 373, p. 20-30.

Hatcher, R.D., and Merschat, A.J., 2006. The Appalachian Inner Piedmont: an exhumed, strike-parallel, tectonically forced orogenic channel. In: Law, R.D., Searle, M.P. and Godin, L. (eds.) Channel Flow, Ductile Extrusion and Exhumation in Continental Collision Zones. Geological Society of London, Special Publications, v. 268, p. 517-541.

Hier-Majumder, S., Ricard, Y., and Bercovici, D., 2006, Role of grain boundaries in magma migration and storage. Earth and Planetary Science Letters, v. 248, p. 735-749.

Hilley, G.E., Bürgmann, R., Zhang, P.-Z., and Molnar, P., 2005. Bayesian inference of plastosphere viscosities near the Kunlun Fault, northern Tibet. Geophysical Research Letters, v. 32, L01302, doi:10.1029/2004GL021658.

Holtzman, B.K., Groebner, N.J., Zimmerman, M.E., Ginsberg, S.B., and Kohlstedt, D.L., 2003. Stress-driven melt segregation in partially molten rocks. Geochemistry, Geophysics, Geosystems, v. 4, doi:10.1029/2001GC000258.

Holtzman, B.K., and Kohlstedt, D.L., 2007. Stress-driven melt segregation and strain partitioning in partially molten rocks: effects of stress and strain. Journal of Petrology, v. 48, p. 2379-2406.

Jamieson, R.A., Beaumont, C., Fullsack, P, and Lee, B., 1998. Barrovian regional metamorphism: where's the heat? In: Treloar, P.J., and O'Brien, P.J. (eds.) What Drives Metamorphism and Metamorphic Reactions? Geological Society of London, Special Publications, v. 138, p. 23-51.

Jamieson, R.A., Beaumont, C., Medvedev, S., and Nguyen, M.H., 2004. Crustal channel flows: 2. Numerical models with implications for metamorphism in the Himalayan-Tibetan orogen. Journal of Geophysical Research, v. 109, B06407, doi:10.1029/2003JB002811.

Jamieson, R.A., Beaumont, C., Nguyen, M.H., and Grujic, D., 2006. Provenance of the Greater Himalayan Sequence and associated rocks: predictions of channel flow models. In: Law, R.D., Searle, M.P. & Godin, L. (eds.) Channel Flow, Ductile Extrusion and Exhumation in Continental Collision Zones. Geological Society of London, Special Publications, v. 268, p. 165-182.

Jamieson, R.A., Unsworth, M.J., Harris, N.B.W., Rosenberg, C.L., and Schulmann, K., 2011. Crustal melting and the flow of mountains. Elements, v., 7, p. 263-260.

Jessell, M.W., Kostenko, O., and Jamtveit, B., 2003. The preservation potential of microstructures during static grain growth. Journal of Metamorphic Geology, v. 21, p. 481-491.

Jones, R. R., Holdsworth, R. E., Hand, M. and Goscombe, B. 2006. Ductile extrusion in continental collision zones: ambiguities in the definition of channel flow and its identification in ancient orogens. In: Law, R. D., Searle, and M. P. Godin, L. (eds.) Channel Flow, Ductile Extrusion and Exhumation in Continental Collision Zones. Geological Society of London, Special Publications, v. 268, p. 201-219.

Kind, R., Ni, J., Zhao, W., Wu, J., Yuan, X., Zhao, L., Sandvol, E., Reese, C., Nabelek, J., and Hearn, T., 1996. Evidence from earthquake data for a partially molten crustal layer in southern Tibet. Science, v. 274, p. 1692- 1694.

Kohlstedt, D.L., 1992. Structure, rheology and permeability of partially molten rocks at low melt fractions. In: Morgan, J.P., Blackman, D.K., and Sinton, J.M. (eds.) Mantle Flow and Melt Generation at Mid-Ocean Ridges. American Geophysical Union, Geophysical Monograph, v. 71, p. 103-121.

Kohlstedt, D.L., Evans, B., and Mackwell, S.J., 1995. Strength of the lithosphere: constraints imposed by laboratory experiments. Journal of Geophysical Research, v. 10, p. 17587-17602.

Kriegsman, L.M., 2001. Partial melting, partial melt extraction and partial back reaction in anatectic migmatites. Lithos, v. 56, p. 75-96.

Laitala, M., 1970. Geological map of Finland, Pre-Quaternary Rocks, sheet 2011 (Hanko), 1:100000. Geological Survey of Finland.

Langille, J., Lee, J., Hacker, B., and Seward, G., 2010. Middle crustal ductile deformation patterns in southern Tibet: Insights from vorticity studies in Mabja Dome. Journal of Structural Geology, v. 32, p. 70-85.

Larson, K.P., and Godin, L., 2009. Kinematics of the Greater Himalayan sequence, Dhaulagiri Himal: implications for the structural framework of central Nepal. Journal of the Geological Society of London, v. 166, p. 25-43.

Lavallée, Y., Hess, K.-U., Cordonnier, B., and Dingwell, D.B., 2007. Non-Newtonian rheological law for highly crystalline dome lavas. Geology, v. 35, p. 843-846.

Leloup P.H., Mahéo, G., Arnaud, N., Kali, E., Boutonnet, E., Liu, D., Xiaohan, L., and Haibing, L., 2010. The South Tibet detachment shear zone in the Dinggye area: Time constraints on extrusion models of the Himalayas. Earth and Planetary Science Letters, v. 292, p. 1-16.

Le Pourhiet, L., Huet, B., May, D.A., Labrousse, L., and Jolivet, L., 2012. Kinematic interpretation of the 3D shapes of metamorphic core complexes. Geochemistry, Geophysics, Geosystems, v. 13, doi:10.1029/2012GC004271.

Long, S., and McQuarrie, N., 2010. Placing limits on channel flow: Insights from the Bhutan Himalaya. Earth and Planetary Science Letters, 290, 375-390.

Makovsky, Y., and Klemperer, S.L., 1999. Measuring the seismic properties of Tibetan bright spots: Evidence for free aqueous fluids in the Tibetan middle crust. Journal of Geophysical Research, v. 104, p. 10795-10825.

Menegon, L., Nasipuri, P. Stünitz, H., Behrens, H., and Ravna, E., 2011. Dry and strong quartz during deformation of the lower crust in the presence of melt. Journal of Geophysical Research, v. 116, B10410, doi:10.1029/2011JB008371.

Miller, R.B., Paterson, S.R., Lebit, H., Alsleben, H., and Lüneburg, C., 2006. Significance of composite lineations in the mid- to deep crust: a case study from the North Cascades, Washington. Journal of Structural Geology, v. 28, p. 302-322.

Mottram, C.M., Warren, C.J., Regis, D., Roberts, N.M.W., Harris, N.B.W., Argles, T.W., and Parrish, R.R., 2014. Developing an inverted Barrovian sequence; insights from monazite petrochronology. Earth and Planetary Science Letters, v., 403, p. 418-431.

Nelson, K.D., Zhao, W., Brown, L.D., Kuo, J., Che, J., Liu, X., Klemperer, S.L., Makovsky, Y., Meissner, R., Mechie, J., Kind, R., Wenzel, F., Ni, J., Nabelek, J., Chen. L., Tan, H., Wie. W., Jones, A.G., Brooker, J., Unsworth, M., Kidd, W.S.F., Hauck, M., Alsdorf, D., Ross, A., Cogan, M., Wu, C., Sandvol, E.A., and Edwards, M., 1996. Partially molten middle crust beneath southern Tibet; synthesis of Project INDEPTH results. Science, v. 274, p. 1684-1688.

Paterson, M.S., 1987. Problems in the extrapolation of laboratory rheological data. Tectonophysics, v. 133, p. 33-43.

Petford, N., Cruden, A.R., McCaffrey, K.J.W., and Vigneresse, J.-L., 2000. Granite magma formation, transport and emplacement in the Earth's crust. Nature, v. 408, p. 669-673.

Platt, J.P., Behr, W.M., and Cooper, F.J., 2015. Metamorphic core complexes: windows into the mechanics and rheology of the crust. Journal of the Geological Society of London, v. 172, p.9-27.

Ramsay, J.G., 1962. Interference patterns produced by the superposition of folds of similar type. Journal of Geology, v. 70, p. 466-481.

Renner, J., Evans, B., and Hirth, G., 2000. On the rheologically critical melt fraction. Earth and Planetary Science Letters, v.181, p. 585-594.

Rey, P.F., Teyssier, C., Kruckenberg, S.C., and Whitney, D.L., 2011. Viscous collision in channel explains double domes in metamorphic core complexes. Geology, v. 39, p. 387-390.

Rey, P.F., Teyssier, C., Whitney, D.L. 2009. The role of partial melting and extensional strain rates in the development of metamorphic core complexes. Tectonophysics 477, 135-144.

Reynolds, O., 1883. An experimental investigation of the circumstances which determine whether the motion of water shall be direct or sinuous, and of the law of resistance in parallel channels. Philosophical Transactions of the Royal Society, v. 174, p. 935–982.

Ridley, J., 1982. Arcuate lineation trends in a deep level, ductile thrust belt, Syros, Greece. Tectonophysics, v. 88, p. 347-360.

Rosenberg, C.L., and Handy, M.R., 2005, Experimental deformation of partially melted granite revisited: Implications for the continental crust: Journal of Metamorphic Geology, v. 23, p. 19–28.

Royden, L.H., Burchfiel, B.C., King, R.W., Wang, E., Chen, Z., Shen, F., and Liu, Y., 1997. Surface deformation and lower crustal flow in eastern Tibet. Science, v. 276, p. 788-790.

Royden, L.H., Burchfiel, B.C., and van der Hilst, R.D., 2008. The geological evolution of the Tibetan Plateau. Science, v. 321, p. 1054-1058.

Rutter, E.H., Brodie, K.H., and Irving, D.H., 2006. Flow of synthetic, wet, partially molten “granite” under undrained conditions: An experimental study. Journal of Geophysical Research, v. 111, doi:10.1029/2005JB004257.

Searle, M., 2013. Crustal melting, ductile flow, and deformation in mountain belts: Cause and effect relationships. Lithosphere, v. 5, p. 547-554.

Searle, M.P., Law, R.D., and Jessup, M.J., 2006. Crustal structure, restoration and evolution of the Greater Himalaya in Nepal-South Tibet: implications for channel flow and ductile extrusion of the middle crust. In: Law, R. D., Searle, and M. P. Godin, L. (eds.) Channel Flow, Ductile Extrusion and Exhumation in Continental Collision Zones. Geological Society of London, Special Publications, v. 268, p. 201-219.

Skyttä, P., and Mänttäri, I., 2008. Structural setting of late Svecofennian granites and pegmatites in Uusimaa Belt, SW Finland: Age constraints and implications for crustal evolution. Precambrian Research, v. 164, p. 86-109.

Stevenson, R.J., Dingwell, D.B., Webb, S.L., and Sharp, T.G., 1996, Viscosity of microlite-bearing rhyolitic obsidians: An experimental study. Bulletin of Volcanology, v. 58, p. 298–309.

Suominen, V., 1987. Geological map of Finland, Pre-Quaternary Rocks, sheet 1032 (Korpo), 1:100000. Geological Survey of Finland.

Sygala, A., Bukowska, M., and Janoszek, T., 2013. High temperature versus geomechanical parameters of selected rocks - the present state of research. Journal of Sustainable Mining, v. 12, p. 45-51.

Thompson, A.B. and Connolly, J.A.D., 1995. Melting of the continental crust: some thermal and petrological constraints on anatexis in continental collision zones and other tectonic settings. Journal of Geophysical Research, v. 100, p. 15565-15579.

Tikoff, B., and Greene, D., 1997. Stretching lineations in transpressional shear zones: an example from the Sierra Nevada Batholith, California. Journal of Structural Geology, v. 19, p. 29-39.

Torvela, T., Moreau, J., Butler, R.W.H., Korja, A. & Heikkinen, P., 2013. The mode of deformation in the orogenic mid-crust revealed by seismic attribute analysis. Geochemistry, Geophysics, Geosystems, v. 14, p. 1069-1086.

Trap, P., Faure, M., Lin, W., Augier, R., and Fouassier, A., 2011. Syn-collisional channel flow and exhumation of Paleoproterozoic high pressure rocks in the Trans-North China Orogen: The critical role of partial-melting and orogenic bending. Gondwana Research, v. 20, p. 498-515.

Unsworth, M.J., Jones, A.G., Wei, W., Marquis, G., Gokarn, S.G., Spratt, J.E., and the INDEPTH-MT team, 2005. Crustal rheology of the Himalayan and Southern Tibet inferred from magnetotelluric data. Nature, v. 438, p. 78-81.

Vanderhaeghe, O., and Teyssier, C., 2001a. Crustal-scale rheological transitions during late-orogenic collapse. Tectonophysics, v. 335, p. 211-228.

Vanderhaeghe, O., and Teyssier, C., 2001b. Partial melting and flow of orogens. Tectonophysics, v. 342, p. 451-472.

Vanderhaeghe, O., 2009. Migmatites, granites and orogeny: Flow modes of partially-molten rocks and magmas associated with melt/solid segregation in orogenic belts. Tectonophysics, v. 477, p. 119-134.

Van der Molen, I., and Paterson, M.S., 1979. Experimental deformation of partially-melted granite. Contributions to Mineralogy and Petrology, v. 70, p. 299-318.

Vigneresse, J.L., Barbey, P., and Cuney, M., 1996, Rheological transitions during partial melting and crystallisation with application to felsic magma segregation and transfer. Journal of Petrology, v. 57, p. 1579-1600.

Wang, J.N., Hobbs, B.E., Ord, A., Shimamoto, T., and Toriumi, M., 1994. Newtonian dislocation creep in quartzites: implications for the rheology of the lower crust. Science, v. 365, p. 1204-1206.

Wang, C., Gao, R., Yin, A., Wang, H., Zhang, Y., Guo, T., Li, Q., and Li, Y., 2011. A mid-crustal strain-transfer model for continental deformation: A new perspective from high-resolution deep seismic-reflection profiling across NE Tibet. Earth and Planetary Science Letters, v. 306, p. 279-288.

Weijermars R., and Schmeling, H., 1986. Scaling of Newtonian and non-Newtonian fluid dynamics without inertia for quantitative modelling of rock flow due to gravity (including the concept of rheological similarity). Physics of the Earth and Planetary Interiors, v. 43, p. 316-330.

Whitney, D.L., Teyssier, C., and Vanderhaeghe, O., 2004. Gneiss domes and crustal flow. In: Whitney, D.L, Teyssier, C., and Siddoway, C.S., Gneiss domes in orogeny: Boulder, Colorado. Geological Society of America Special Paper, v. 380, p. 15–33.

Whitney, D.L., Teyssier, C., Rey, P., and Buck, W.R., 2013. Continental and oceanic core complexes. Geological Society of America Bulletin, v. 125, p. 273-298.

Williams, P.F. and Jiang, D., 2005. An investigation of lower crustal deformation: Evidence for channel flow and its implications for tectonics and structural studies. Journal of Structural Geology, v. 27, p. 1486-1504.

Zhang, P.-Z., Shen, Z., Wang, M., Gan, W., Bürgmann, R., Molnar, P., Wang, Q., Niu, Z., Sun, J., Wu, J., Hanrong, S., and Xinzhao, Y., 2004. Continuous deformation of the Tibetan Plateau from global positioning system data. Geology, v. 32, p. 809-812.

Figure captions

Figure 1. Principle of the channel flow model underneath an orogen with a continental plateau, such as the Himalayan-Tibetan system (modified from Vanderhaeghe, 2009, based on Grujic et al. 2002). Channel flow encompasses elements of both Couette and Poiseuille flow types, the relative particle velocity paths of which are also illustrated. The relative contribution of Couette vs. Poiseuille varies trough time and space within the channel itself, but overall relative displacement in opposite directions of the rigid boundaries is necessary (one of the first-order characteristics for mid-crustal channel flow discussed by e.g. Godin et al., 2008). Fg = gravitational force, Ft = basal traction force, Fc = the horizontal compression force.

Figure 2. Examples of the Gibson et al. (2009) flow model for planar Couette flow of a viscous fluid with a random initial internal organisation, within a relatively high aspect ratio channel between shearing rigid plates (time steps taken from a video on www.channelflow.org, accessed on 5 May 2015). The top surface is the horizontal "map" view, the sides of the diagram are "cross sections" at different levels with respect to the "map" surface. The arrows within the channel represent material flow vectors (i.e. the arrow length is proportional to flow speed/strength). The colours enhance the flow direction visualisation, with red colours indicating flow toward the upper plate shear direction (toward top right of the model), and blue indicating flow toward the lower plate shearing direction (toward bottom left). The cyclical nature of the flow for the modelled fluid is evident: the random initial condition (A) develops into a weak turbidity pattern (B), which settles down into elongate "ridge flow" patterns (C), that become somewhat unstable with time, again developing some weak turbidity (D). The model is for viscous fluid but the viscosity is still much lower than would be expected for mid-crustal material: these models are not directly applicable to the mid-crustal channel flow, but are used here to give some visual insights as to the variability of outcrop patterns/structures that may result (see Fig. 3 and the text).

Figure 3. Geometric thought exercises, based on Figure 2B, of the effects of channel flow on initially A) horizontal and B) moderately dipping layering (pre-

flow dip direction/dip c. 100/30). In A), the layer-parallel flow (with local perturbations) leads to recumbent (sheath) folds with c. N-S fold axes, and to formation of elongate, shear-parallel domes with doubly vergent, E-W trending axial traces; in B), flow is not layer-parallel but overturned folds with c. N-S trending axes form especially in places of convergence of opposite flow directions; most folds form due to local variations in flow rate and show E-plunging fold axes. In both cases, stretching lineations are expected to form dominantly along the fold/dome axial traces and along shear zone kinematic vectors. The layering/foliation steepens toward the edges of the channel as can be seen in the "east-west" oriented cross sections along the model edges (see also the inset for the changing foliation/layering dips). Theoretical stereonets of the expected overall patterns of dominant foliation/layering (S), fold axes (F), and stretching lineations (L) are shown. These extremely simplified models illustrate how the initial geometry/structural grain has a significant impact on the resulting outcrop geometries. Extrapolating to orogenic scales and assuming a channel thickness of 10 km, the horizontal extent of the model is c. 80 x 80 km.

Figure 4. Examples of outcrop patterns interpreted to represent mid-crustal channel flow, mainly based on foliation/fold patterns and stretching lineations: modified from A) Hatcher and Merschat (2006), showing the form line map of foliations (with teeth indicating dip direction), a map of mineral lineations, and a flow model based on the geological mapping and lineation data; B) the main map and stereonets from Cagnard et al. (2006), the map showing outcrop traces of metamorphic layering (most prominent within the migmatites exposed between the subhorizontal syn-orogenic microcline granite sheets), and the stereonets giving examples of attitudes of typical stretching lineations that are steep within the shear zones (black lines) and more scattered but E-W to NE-SW trending elsewhere. Cagnard et al. (2006) use these data and the lineation map (smaller) covering approximately the same area (from Ehlers et al., 1993; trajectories of stretching lineations dipping mostly <30°) to suggest a mid-crustal palaeochannel for southern Finland (the block diagram). The location of Figure 6 is shown in the lineation map; and C) Trap et al., 2011 with foliation traces within the HPB and stereonets summarizing the D2 structures interpreted to reflect mid-crustal flow within the HPB. The aim of this figure is to illustrate that various different outcrop

patterns and geometries, and especially the foliation-lineation relationships, have been used to infer channel flow. See text for discussion.

Figure 5. Examples of outcrop patterns that are similar to those in Figure 4, but have not been used to infer channel flow; instead, other mechanisms for their formation are suggested by the authors. Modified from A) Ridley, 1982, showing an arcuate pattern of the dominant stretching lineations (with additional glaucophane lineations at lowermost crustal levels also shown) in the ductile lower crust exposed in Syros, Greece, and lineation-parallel foliations/lithological unit trends (inset), interpreted to represent the subhorizontal displacement of a ductile lower crustal thrust sheet; B) Chardon et al. (2009, 2011) from the Neoarchean orogen of the Dharwar craton (India). The geometric relationships of the doubly plunging lineations (L1 and L2), F2 fold axes perpendicular to shortening, and dome- or lens-like foliation patterns are interpreted to represent lateral constrictional flow rather than channel flow. The two block models on the left are for 1) decoupled, highly buoyant, and weak and 2) coupled lower crust; both showing approximate strain ellipsoid shapes); and C) Denele et al. (2007) with doubly plunging shallow lineations and folded foliation patterns in the Hospitalet Massif, the Axial Zone of the Pyrenees. The patterns are interpreted to reflect eastward shearing and subsequent/simultaneous folding. The aim of this figure is to show alternative explanations of how "channel flow patterns" could form: although some examples are from orogen types, metamorphic grades, and scales different to the Himalayan-Tibetan middle crust, the basic geometric and kinematic principles should be applicable.

Figure 6. A simplified geological map from the Turku archipelago, southwestern Finland (see Fig. 4. for location). Based on field work by the author, and on Laitala (1970), Edelman (1954, 1973), and Suominen (1987). Representative lineations are marked along with lineation trajectories and migmatitic foliation trends. There are thousands of small islands and skerries in the archipelago, only the largest (groups) of islands are outlined on the inset map. The W-E striking Rosala-Jurmo high-strain zone (RJZ) is shaded. The stereonets compile the migmatitic foliations (S1-2; see text), fold axes (F; interpreted to be mostly F2 folds as described in the text), and mineral, stretching, and crenulation lineations

(L2) observed in the field. Contour plots for S and F = 1%, 2%, 4%, 8% and 16%; and for L = 1%, 2%, 4% and 8%. The outcrop patterns greatly resemble some patterns interpreted as channel flow (Figs. 4B, C) but could also be claimed to be analogous to Fig. 5C and partly also Fig. 5B. Note especially the foliation-lineation-fold relationships that are very similar to both Fig. 4C and Fig. 5C. See text for further discussion.

Figure 7. Modified from A) Whitney et al. (2004) and B) Rey et al. (2011). A) shows a schematic sketch of a gneiss dome with some characteristic feature; the theoretical relationships between lateral channel flow and vertical diapiric flow; the conceptual expected PTt (pressure-temperature-time) paths for locations A -> A' and B -> B' ("active doming"), and A -> A'' and B -> B'' ("passive doming") in channel flow vs. diapiric flow; in B), the results of a numerical experiment by Rey et al. (2011) illustrate strain distribution and flow paths in extensional gneiss dome formation; note the very different patterns in the internal dome structure depending on the observation depth, and the longevity and the rate of dome formation. Note also that only limited lateral "channel" flow at mid-crustal depths is needed for doming to occur.

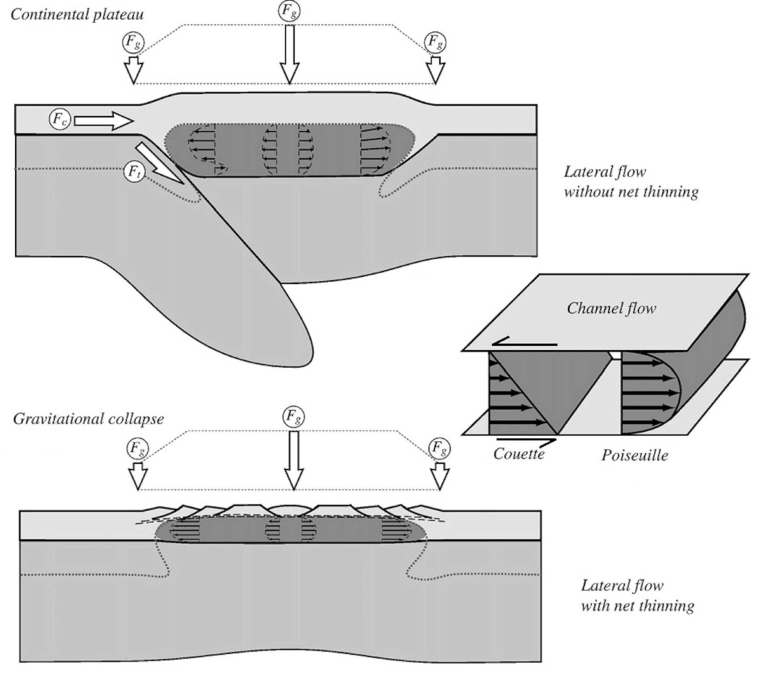
Continental plateau
F_g
F_g
F_g
F_c
F_t
Lateral flow
without net thinning
Channel flow
Couette
Poiseuille
Gravitational collapse
F_g
F_g
F_g
Lateral flow
with net thinning

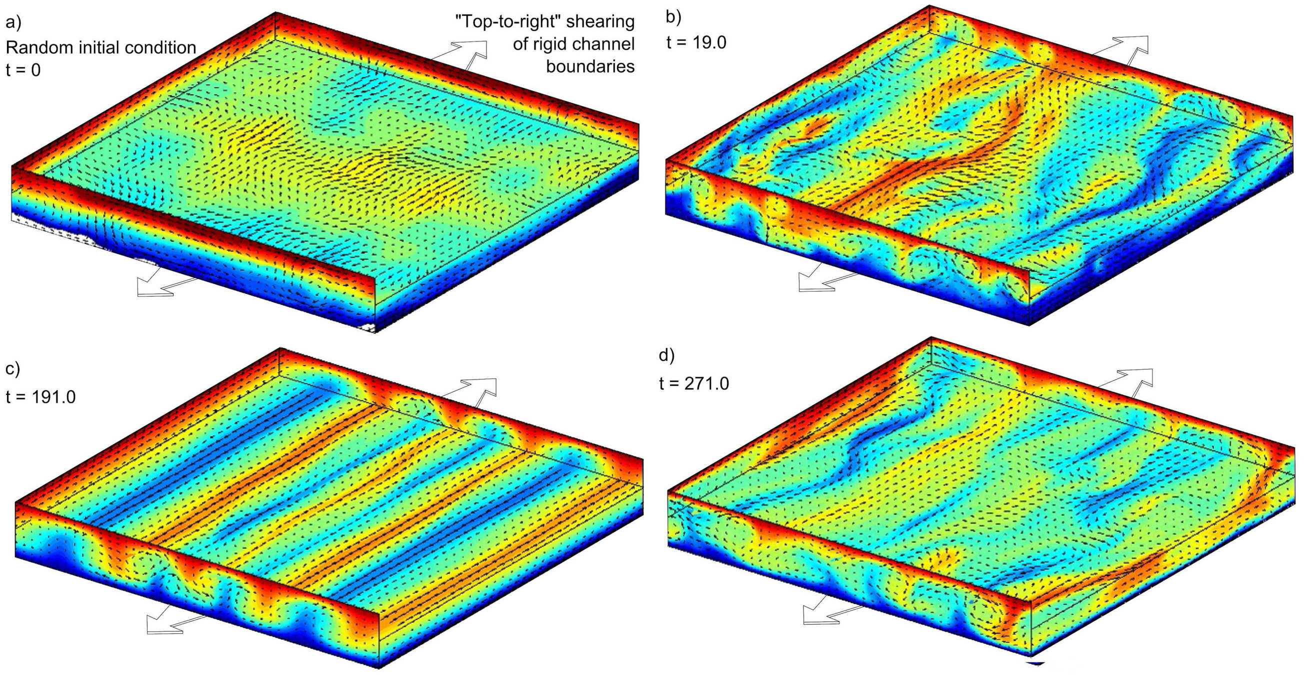
a)
Random initial condition
t = 0
"Top-to-right" shearing
of rigid channel
boundaries
b)
t = 19.0
c)
t = 191.0
d)
t = 271.0

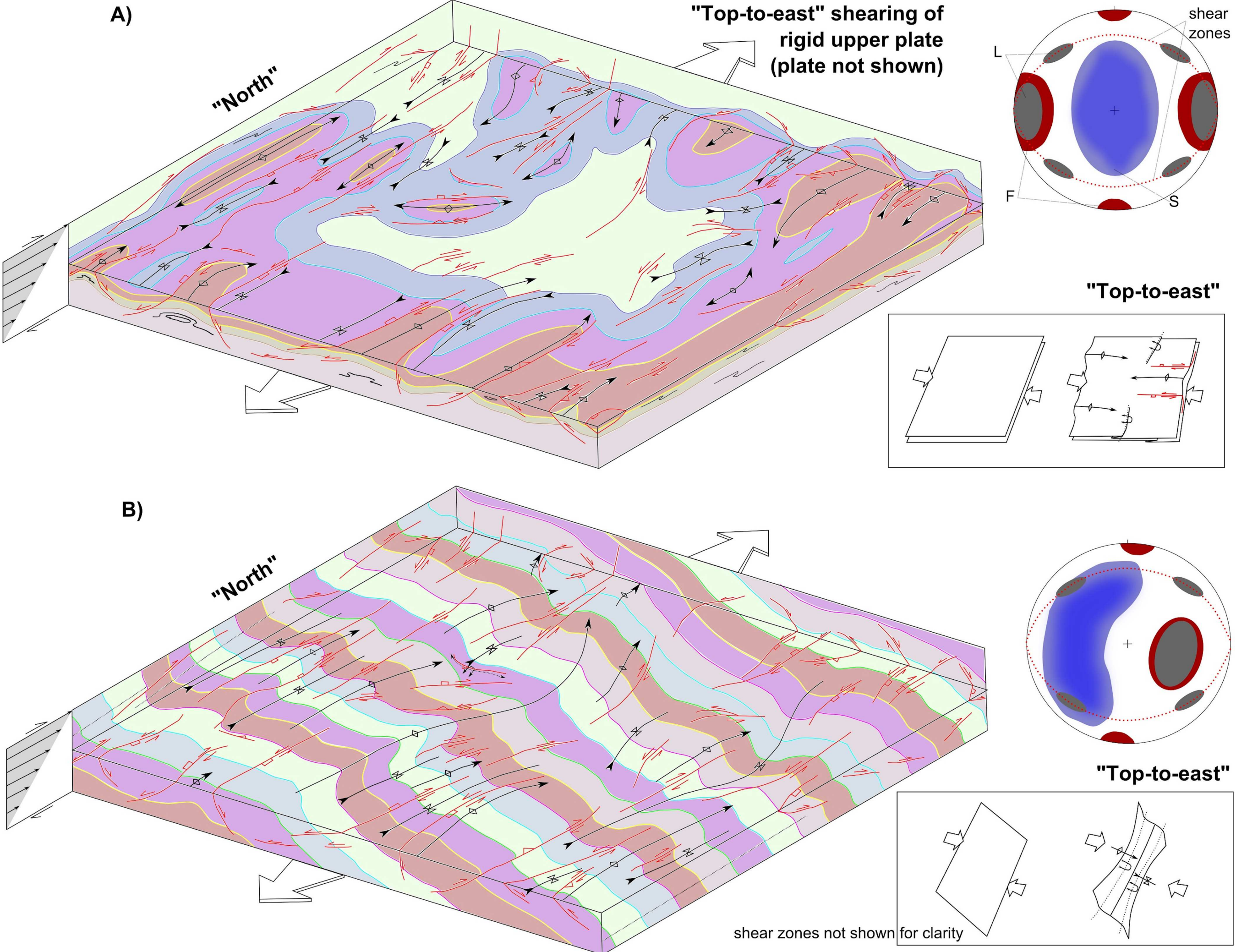
A)
"Top-to-east" shearing of
rigid upper plate
(plate not shown)
"North"
shear
zones
L
F
S
"Top-to-east"
B)
"North"
"Top-to-east"
shear zones not shown for clarity

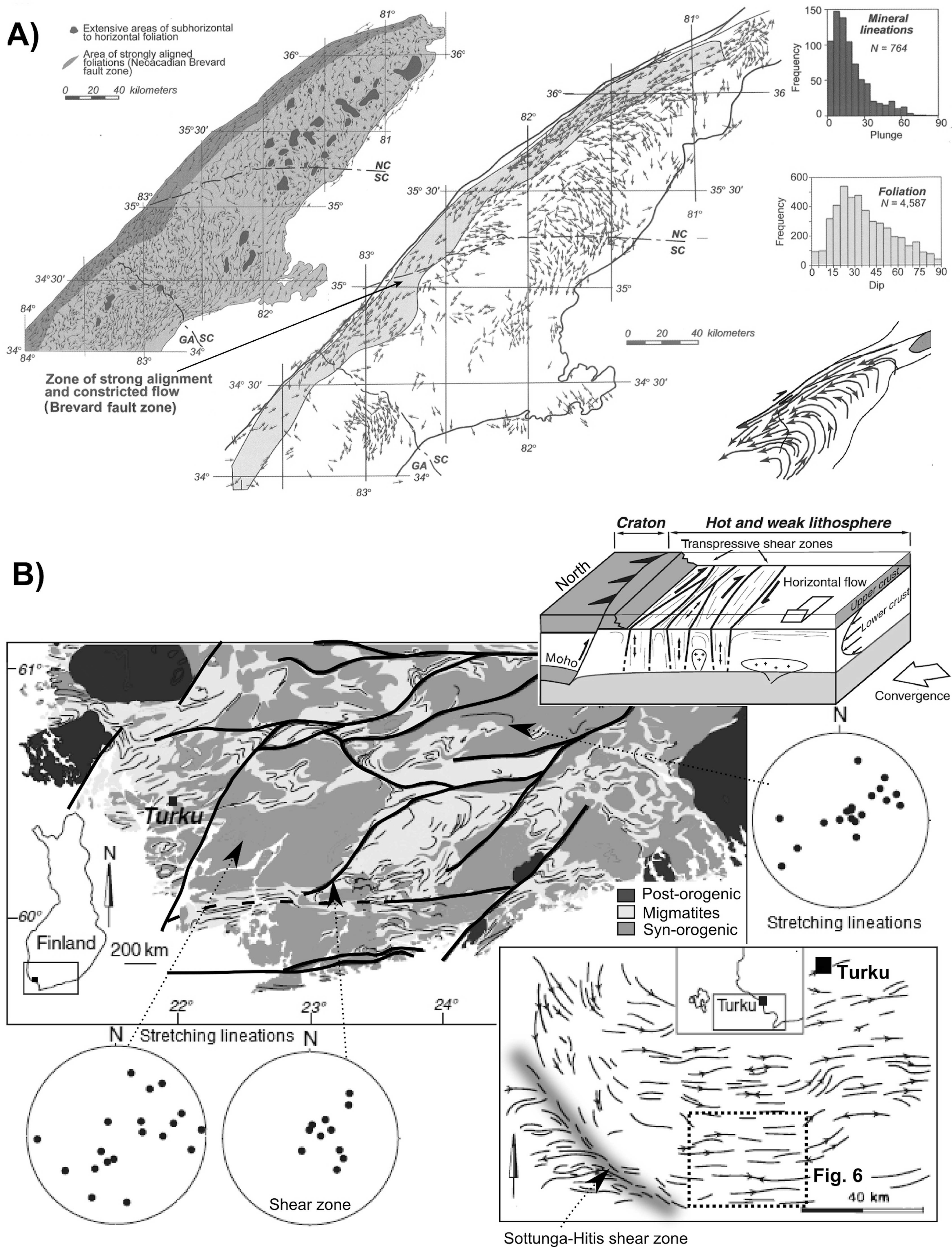
A)
Extensive areas of subhorizontal to horizontal foliation
Area of strongly aligned foliations (Neoacadian Brevard fault zone)
0 20 40 kilometers
NC
SC
GA
SC
Zone of strong alignment and constricted flow (Brevard fault zone)
Mineral lineations
N = 764
Frequency
Plunge
Foliation
N = 4,587
Frequency
Dip
0 20 40 kilometers
B)
Craton
Hot and weak lithosphere
Transpressive shear zones
North
Horizontal flow
Upper crust
Lower crust
Moho
Convergence
Turku
Finland
200 km
Post-orogenic
Migmatites
Syn-orogenic
Stretching lineations
Stretching lineations
Shear zone
Turku
Turku
Fig. 6
40 km
Sottunga-Hitis shear zone

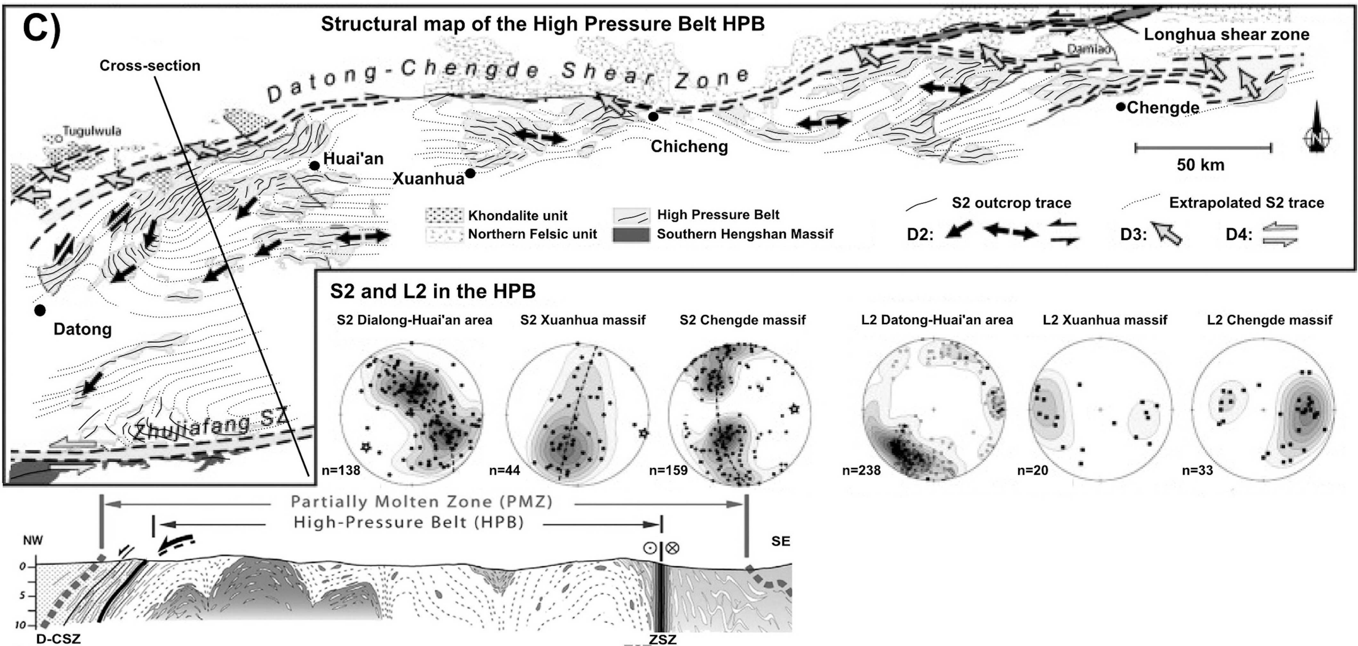
C)
Structural map of the High Pressure Belt HPB
Cross-section
Datong-Chengde Shear Zone
Longhua shear zone
Damiao
Tugulwula
Huai'an
Xuanhua
Chicheng
Chengde
Datong
Zhujiafang SZ
50 km
Khondalite unit
Northern Felsic unit
High Pressure Belt
Southern Hengshan Massif
S2 outcrop trace
Extrapolated S2 trace
D2:
D3:
D4:
S2 and L2 in the HPB
S2 Dialong-Huai'an area
S2 Xuanhua massif
S2 Chengde massif
L2 Datong-Huai'an area
L2 Xuanhua massif
L2 Chengde massif
n=138
n=44
n=159
n=238
n=20
n=33
Partially Molten Zone (PMZ)
High-Pressure Belt (HPB)
NW
SE
0
5
10
D-CSZ
ZSZ

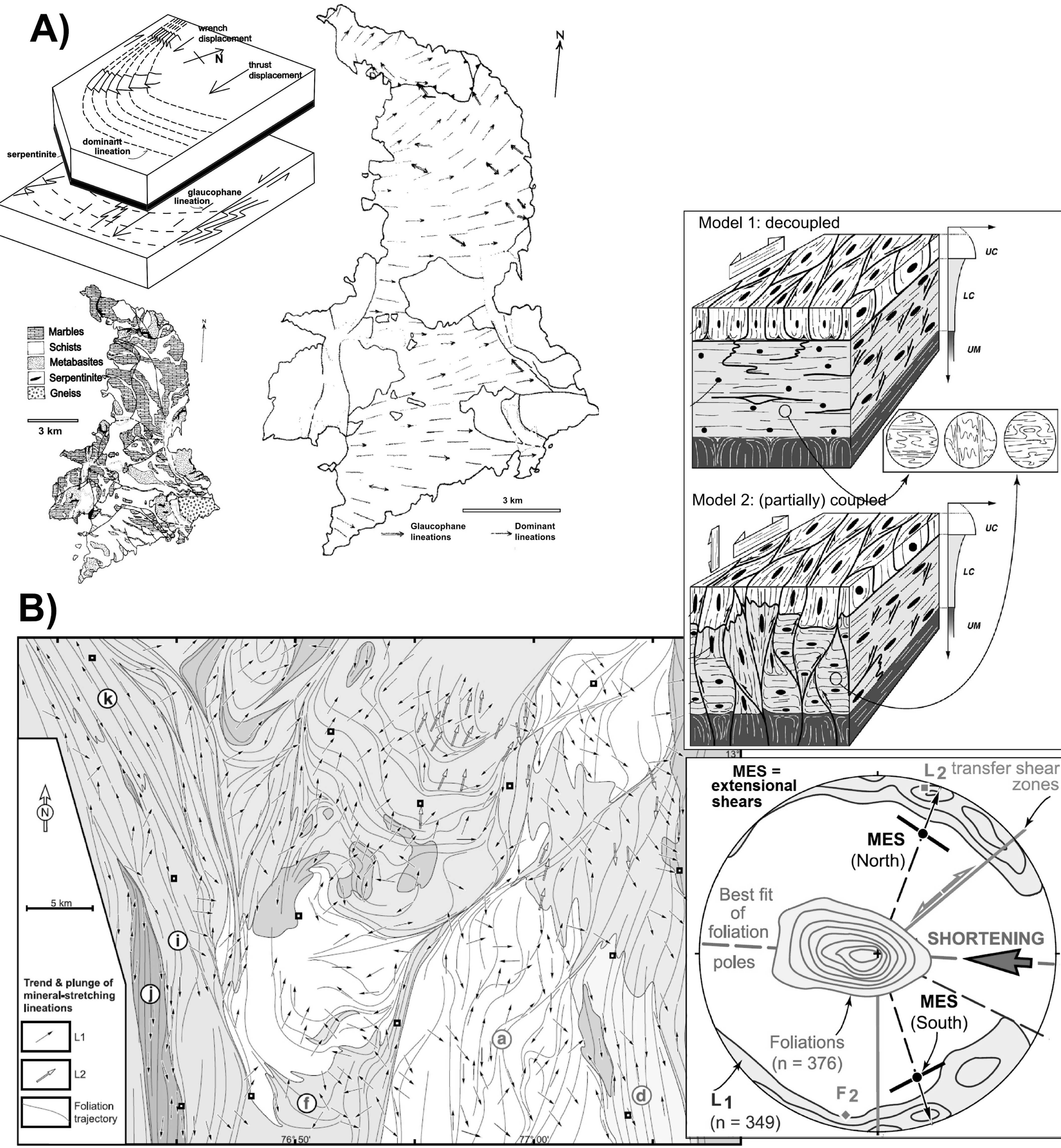
A)
wrench displacement
N
thrust displacement
dominant lineation
serpentinite
glaucophane lineation
Marbles
Schists
Metabasites
Serpentinite
Gneiss
3 km
N
3 km
Glaucophane lineations
Dominant lineations
Model 1: decoupled
UC
LC
UM
Model 2: (partially) coupled
UC
LC
UM
B)
k
N
5 km
i
j
Trend & plunge of mineral-stretching lineations
L1
L2
Foliation trajectory
f
a
d
76° 50'
77° 00'
13°
MES = extensional shears
L 2
transfer shear zones
MES (North)
Best fit of foliation poles
SHORTENING
MES (South)
Foliations (n = 376)
L 1 (n = 349)
F 2

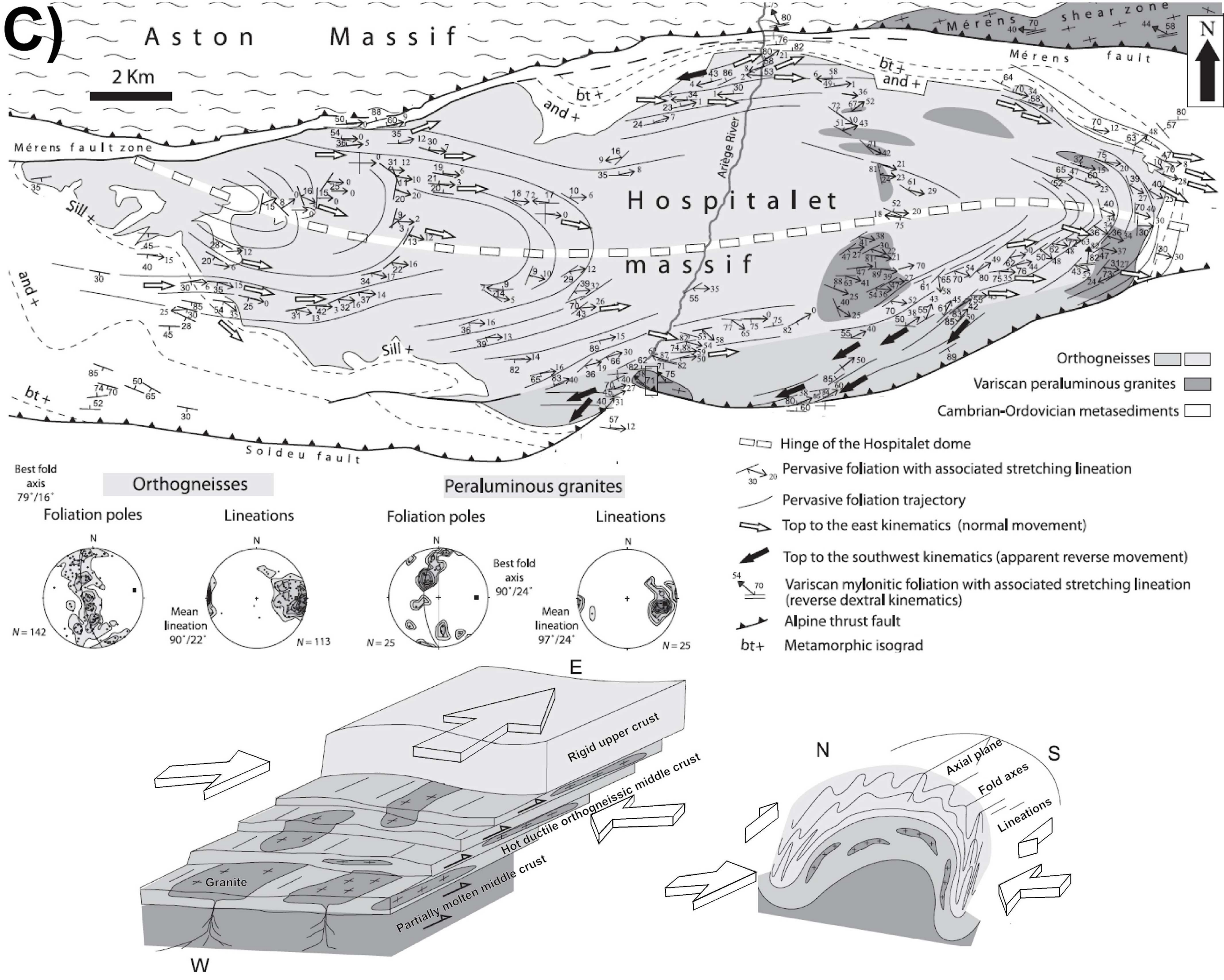
C)
Aston Massif
2 Km
N
Mérens shear zone
Mérens fault
Mérens fault zone
bt +
and +
Ariège River
Hospitalet massif
Sill +
Soldeu fault
Orthogneisses
Variscan peraluminous granites
Cambrian-Ordovician metasediments
Hinge of the Hospitalet dome
Pervasive foliation with associated stretching lineation
Pervasive foliation trajectory
Top to the east kinematics (normal movement)
Top to the southwest kinematics (apparent reverse movement)
Variscan mylonitic foliation with associated stretching lineation (reverse dextral kinematics)
Alpine thrust fault
bt+ Metamorphic isograd
Best fold axis 79°/16°
Orthogneisses
Foliation poles
Lineations
N = 142
Mean lineation 90°/22°
N = 113
Peraluminous granites
Foliation poles
Best fold axis 90°/24°
N = 25
Lineations
Mean lineation 97°/24°
N = 25
E
W
Rigid upper crust
Hot ductile orthogneissic middle crust
Partially molten middle crust
Granite
N
S
Axial plane
Fold axes
Lineations

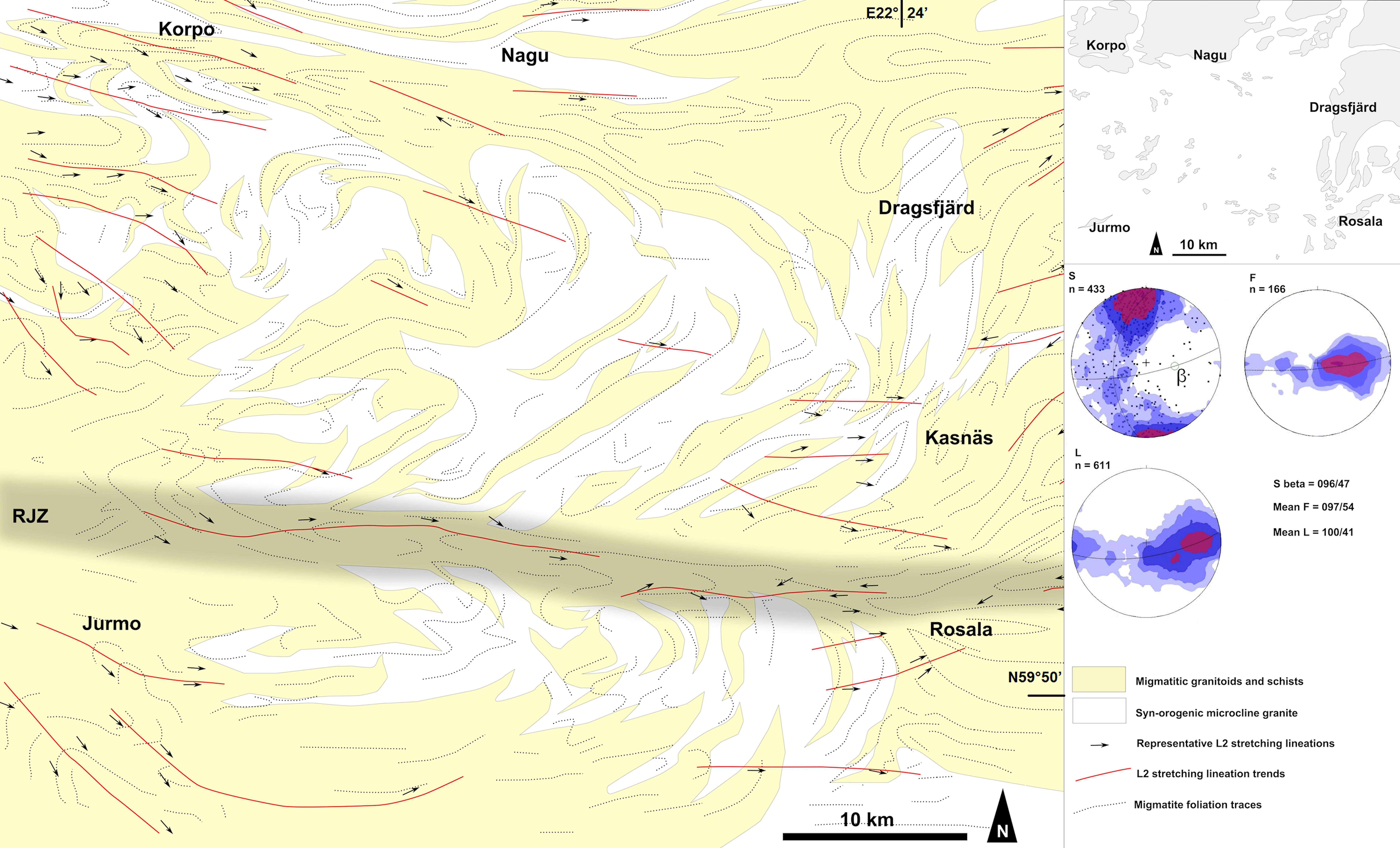
E22° 24'
Korpo
Nagu
Dragsfjärd
Kasnäs
RJZ
Jurmo
Rosala
N59°50'
10 km
N
Korpo
Nagu
Dragsfjärd
Jurmo
Rosala
10 km
S
n = 433
β
F
n = 166
L
n = 611
S beta = 096/47
Mean F = 097/54
Mean L = 100/41
Migmatitic granitoids and schists
Syn-orogenic microcline granite
Representative L2 stretching lineations
L2 stretching lineation trends
Migmatite foliation traces

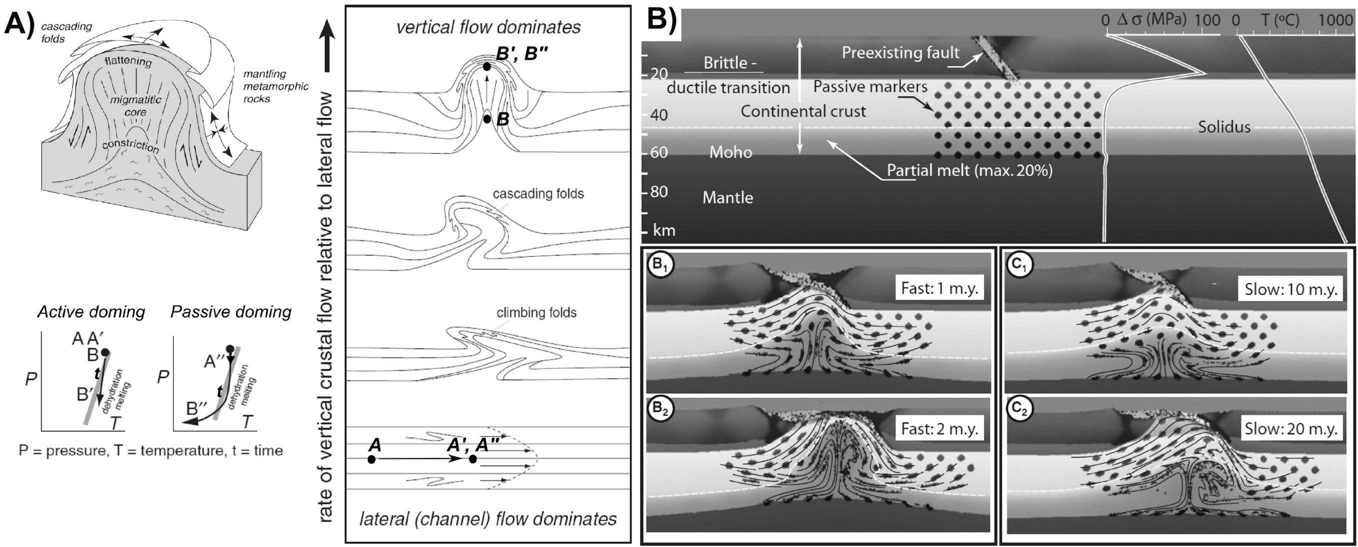
A)
cascading folds
flattening
mantling metamorphic rocks
migmatitic core
constriction
Active doming
Passive doming
A A′
B
t
B′
dehydration melting
P
T
A″
B″
P = pressure, T = temperature, t = time
rate of vertical crustal flow relative to lateral flow
vertical flow dominates
B′, B″
B
cascading folds
climbing folds
A
A′, A″
lateral (channel) flow dominates
B)
0 Δσ (MPa) 100
0 T (°C) 1000
Brittle -
ductile transition
Preexisting fault
Passive markers
Continental crust
Solidus
Moho
Partial melt (max. 20%)
Mantle
20
40
60
80
km
B1
Fast: 1 m.y.
C1
Slow: 10 m.y.
B2
Fast: 2 m.y.
C2
Slow: 20 m.y.